

Quantum neural ODEs and PDEs

Yu Cao,^{1, 2, 3, *} Shi Jin,^{1, 2, 3} and Nana Liu^{1, 2, 3, 4, †}

¹*Institute of Natural Sciences, Shanghai Jiao Tong University, Shanghai 200240, China*

²*Ministry of Education Key Laboratory in Scientific and Engineering Computing,
Shanghai Jiao Tong University, Shanghai 200240, China*

³*School of Mathematical Sciences, Shanghai Jiao Tong University, Shanghai, 200240, China*

⁴*Global College, Shanghai Jiao Tong University, Shanghai 200240, China.*

(Dated: August 27, 2025)

We present a unified framework called Quantum Neural Ordinary and Partial Differential Equations (QNODEs and QNPDEs) that brings the continuous-time formalism of classical neural ODEs/PDEs into quantum machine learning and quantum control. We define QNODEs as the evolution of finite-dimensional quantum systems, and QNPDEs as infinite-dimensional (continuous-variable) counterparts, governed by generalised Schrödinger-type Hamiltonian dynamics with unitary evolution, coupled with a corresponding loss function. Notably, this formalism permits gradient estimation using an adjoint-state method, facilitating efficient learning of quantum dynamics, and other dynamics that can be mapped (relatively easily) to quantum dynamics. Using this method, we present quantum algorithms for computing gradients with and without time discretisation, enabling efficient gradient computation that would otherwise be less efficient on classical devices.

The formalism subsumes a wide array of applications, including quantum state preparation, Hamiltonian learning, learning dynamics in open systems, and the learning of both autonomous and non-autonomous classical ODEs and PDEs. In many of these applications, we consider scenarios where the Hamiltonian has relatively few tunable parameters, yet the corresponding classical simulation remains inefficient, making quantum approaches advantageous for gradient estimation. This continuous-time perspective can also serve as a blueprint for designing novel quantum neural network architectures, generalising discrete-layered models into continuous-depth models.

I. INTRODUCTION

The interplay between the study of classical dynamical systems and machine learning has been a fruitful one and holds much promise. The theory of dynamical systems provides a mathematical framework to study the evolution of systems over time, offering insights into stability, chaos, and long-term behavior. Machine learning, particularly in areas like recurrent neural networks and neural ODEs, draws on this theory to model temporal data and learn complex dynamics. Conversely, machine learning aids in discovering governing equations and predicting behaviors in high-dimensional or partially observed dynamical systems. This interplay enriches both fields, enabling data-driven discovery of physical laws and more robust, interpretable learning models.

The key to generalising machine learning algorithms to be amenable to the study of dynamical systems is to generalise discrete-time algorithms into continuous-time ones. In this direction, one notable milestone is the introduction of neural ordinary differential equations (neural ODEs) [1, 2], which has since attracted significant attention. This approach was motivated by the deep connection between ODEs and Residual Networks (ResNet) [3–5]. In parallel, the extension to infinite-dimensional systems is natural, and we refer to these as neural PDEs; however, this concept is often known by other names, such as PDE-Net [6] and physics-informed neural networks (PINN) [7], depending on the specific architecture and training details. Further generalisations have been made to stochastic dynamics, see e.g., [8–11]. Another related framework is the SDE-based diffusion model [12], which unifies earlier discrete-time Markov chain-based generative models [13, 14]. This continuous-time formulation has inspired a surge of research in generative modeling. This continuous-time perspective offers several key advantages: (1) efficient computation enabled by the use of the backpropagation algorithm [15] and classical numerical integrators for dynamical systems; (2) a powerful analytical framework for studying properties such as stability in architecture design [2, 4]; and (3) a

* yucao@sjtu.edu.cn

† nana.liu@quantumlahah.org

unified approach for designing neural network architectures [3–5], providing an alternative to mapping-based architectures.

However, despite the great success of these approaches, there are some fundamental bottlenecks. For example, in the estimation of gradients that is required to train these models via gradient-based methods, the cost of the simulation of these dynamical systems can be large – since for high-dimensional dynamical systems, classical simulation often suffers from the curse of dimensionality, particularly for many-body quantum dynamics. To obviate this, we can use quantum simulation for quantum dynamical systems can avoid this curse of dimensionality [16], and this benefit can also be extended to non-quantum dynamical systems in some scenarios as well.

This motivates us to consider machine learning on quantum devices from the perspective of quantum dynamical systems (an analog perspective on quantum machine learning), which is much less studied compared to its digital counterparts [17–23]. For all quantum algorithms that reply on fundamental quantum mechanics, the most basic dynamical equation is Schrödinger’s equation. Hence, we propose the notion of (closed) quantum neural ODEs and PDEs (QNODEs and QNPDEs) where the state $\rho(t, \theta)$ evolves according to

$$\frac{\partial \rho(t, \theta)}{\partial t} = -i[H(t, \theta), \rho(t, \theta)], \quad \rho(0, \theta) = \rho_0, \quad (1)$$

and $H(t, \theta)$ is a time-dependent Hamiltonian with controllable parameters θ , and there is an associated loss function \mathcal{L} , dependent on the machine learning task. When $\rho(t, \theta)$ is a finite-dimensional quantum system, we refer to this as a (closed) QNODE and if $\rho(t, \theta)$ is an infinite-dimensional quantum system, it is called a (closed) QNPDE. If $\rho(t, \theta)$, instead, obeys open quantum dynamics, then this is an (open) QNODE or QNPDE.

This formalism is natural for quantum machine learning:

- Firstly, this is a very natural formalism for the learning of quantum dynamics itself (namely, Hamiltonian learning [24]), and lends itself easily to the more traditional problems in quantum control and quantum state preparation.
- Secondly, the learning of unknown parameters of other dynamical systems can be made more efficient by the mapping of these dynamical systems to the corresponding quantum dynamics. In particular, we know that for linear and nonlinear ODEs, linear PDEs and certain nonlinear PDEs, there is a very simple mapping possible through Schrödingerisation [25, 26], level set [27] or von Neumann-Koopman formulation [28] that exploits the fully continuous nature of these problems, in both time and space. In this case, the Hamiltonian representation often has a relatively smaller number of unknown parameters (since the form of the problem is known) and this kind of ansatz is much more physically motivated than a generic neural network ansatz.
- Thirdly, in the design of quantum algorithms with the common gate-based methods, those quantum circuits still require the preparation of pulse-level control of the quantum system, which, in fact, runs in continuous time. The so-called discrete-time settings in reality cannot be truly discrete since quantum speed limits [29] fundamentally forbid the instantaneous application of two distinguishable quantum channels one after the other.
- Another motivation is to study the connection to other quantum setups like in quantum neural networks (which run in discrete time steps). Here we have a continuous-depth version which is non-autonomous (i.e., explicit time dependence in the Hamiltonian) and, in principle, the different discretisations can reproduce all other (discrete) architectures for quantum neural networks [30]. Different discretisations can give rise to different architectures. In addition, backpropagation can be performed more directly (a continuous-version of backpropagation). Also, since Hamiltonian dynamics in Eq. (1) is reversible, it is known that for all reversible maps, the loss function gradients can be computed via the adjoint sensitivity method with constant memory cost independent of depth [1, 31]. This decoupling of depth and memory can be important in applications [31].

In our work, we show the feasibility of generalising continuous-time classical backpropagation into the quantum regime and present two algorithms for gradient estimation: one based on partial time discretisation and one that does not require any time discretisation at all. These two algorithms are summarised in Table I, which utilised the back-propagation structure of classical neural ODEs. These algorithms differ from the parameter-shift rule [17, 32–35] for digital quantum devices, which requires quantum measurements using a collection of different parameter values per iteration of the gradient estimate; in our case, the quantum measurements only uses the same set of parameters at each stage and we also don't make restrictions on the Hamiltonian itself. Using the general decomposition of the time-dependent parameterised Hamiltonian

$$H(t, \theta) = \sum_{k=1}^K f_k(t, \theta) H_k \quad (2)$$

where $f_k(t, \theta) \in \mathbb{R}$ and $H_k \neq H_{k'}$ for all $k \neq k'$ are time-independent Hermitian operators, then the cost for gradient estimation depends only on K (and can be as little as $\mathcal{O}(\log K)$), and thus not a priori dependent on the number of tuneable parameters M for θ ; see more discussion in Section IV D.

After a very brief background section, we introduce the QNODE and QNPDE formalism in Section III. In particular, we present the applications of this formalism to learning quantum state preparation and Hamiltonian learning (Section III B), certain learning problems in open quantum systems (Section III C), learning (classical) ODEs/PDEs (Section III D) and learning non-autonomous systems (Section III E). Furthermore, in Section III F we show how this provides a general framework for a large class of quantum neural networks in the continuous-time limit, from which new quantum neural network architectures could emerge from choosing different discretisations. In Section IV we present our quantum algorithms for gradient estimation, using partial time discretisation (Section IV B) and without any time discretisation (Section IV C), then discuss the costs in Section IV D. Some simple numerical examples are in Section V.

TABLE I: Summary of the main quantum gradient estimation algorithms for QNODEs/QNPDEs, see Section IV for more details.

Algorithm	Theorem	Circuit	Treatment of time	Applications
QNODE/QNPDE gradient estimation algorithm (v1)	Theorem 3	Figure 1a	Requires partial time discretisation	<ul style="list-style-type: none"> • State preparation and Hamiltonian learning (closed system (III B); open system (III C)); • Learning ODEs/PDEs (III D); • Learning non-autonomous systems (III E); • Continuous-time framework for QNNs (III F).
QNODE/QNPDE gradient estimation algorithm (v2)	Theorem 5	Figure 1b	Fully continuous in time	

II. BACKGROUND

In this section, we briefly review the notation used in quantum information theory and classical neural ODEs/PDEs in machine learning.

A. Basic notation in quantum information processing

We first summarize the notation for discrete-variable (DV) and continuous-variable (CV) quantum states used in later sections. Quantum information processing is often described in terms of qubits, the quantum analogue of classical bit strings $\{0, 1\}^{\otimes n}$. A qubit uses the eigenbasis $\{|0\rangle, |1\rangle\}$ for the computational basis

and resides in a two-dimensional Hilbert space $\mathcal{H}_{\text{qubit}}$. An n -qubit system lives in a $D = 2^n$ -dimensional Hilbert space, given by the tensor product $(\mathcal{H}_{\text{qubit}})^{\otimes n}$. The corresponding quantum state can be written as $|u\rangle = (1/\|\mathbf{u}\|) \sum_{j=1}^D u_j |j\rangle$, where the normalisation is $\|\mathbf{u}\|^2 = \sum_{j=1}^D |u_j|^2$. This notation can also be used to denote a D -dimensional *qudit* system. Mathematically this is equivalent to a system of $n = \log_2 D$ qubits, but in physical implementation, these are distinct. Both qubits and qudits are discrete-variable (DV) quantum systems.

A continuous-variable (CV) quantum state, or *qumode*, spans an infinite-dimensional Hilbert space $L^2(\mathbb{R})$ [36]. A qumode is the quantum analogue of a continuous classical degree of freedom, such as position or momentum. It is equipped with observables with continuous spectra, such as the position \hat{x} and momentum \hat{p} operators. The eigenbasis $\{|x\rangle\}_{x \in \mathbb{R}}$ consists of eigenstates of \hat{x} , and a qumode can be expressed as $|u\rangle = (1/\|\mathbf{u}\|) \int u(x) |x\rangle dx$, with normalisation $\|\mathbf{u}\|^2 = \int |u(x)|^2 dx$. Integrals \int without terminals denote $\int = \int_{-\infty}^{\infty}$ unless otherwise specified. If $x = (x_1, \dots, x_m)$ then the above represents a system of m qumodes. Although CV quantum information processing is less common than qubit-based approaches, these states are in fact natural for many quantum systems, and is particularly important for the simulation of linear PDEs while preserving continuity in space [25]. The quadrature operators of a qumode are \hat{x} and \hat{p} , where $[\hat{x}, \hat{p}] = i\mathbf{1}$. If we let $|x\rangle$ and $|p\rangle$ denote the eigenvectors of \hat{x} and \hat{p} respectively, then $\langle x|p\rangle = \exp(ixp)/\sqrt{2\pi}$. The position and momentum eigenstates each form a complete eigenbasis so $\int |x\rangle \langle x| dx = \mathbf{1} = \int |p\rangle \langle p| dp$. Here the quantised momentum operator \hat{p} is also associated with the spatial derivative through $i\hat{p}|u\rangle \propto \int \partial u / \partial x |x\rangle dx$. Similarly for the position quadrature, we have the association $\hat{x}|u\rangle \propto \int x u(x) |x\rangle dx$. This is important for associating Hamiltonians acting on qumodes with PDEs [25].

We denote the Hilbert space for the Hamiltonian dynamics as \mathcal{H} (which may be finite- or infinite-dimensional), the adjoint system as \mathcal{H}_{adj} (with the same dimension as \mathcal{H}), and the auxiliary qubit system as \mathcal{H}_{aux} ; see Section IV. We use $\|\cdot\|_p$ to denote the Schatten- p norm of operators; in particular, $\|\cdot\|_\infty$ is the usual operator norm (namely, largest singular value of the operator).

B. Classical neural ODE and PDE

The concept of neural ordinary differential equations (ODEs) was formally introduced in [1, 2], referring to a general parametric family of ODEs of the form:

$$\frac{d}{dt} y(t) = f(y(t), t, \theta), \quad (3)$$

where $f : \mathbb{R}^n \times \mathbb{R} \times \Omega \rightarrow \mathbb{R}^n$ is a (potentially nonlinear) function parameterised by $\theta \in \Omega$, with Ω denoting the domain of parameters. As already discussed in introduction, this framework is motivated by the connection between ODEs and residual networks; see e.g., [3, 4]. For example, applying the Euler discretization with time step Δt yields

$$y_{k+1} = y_k + \Delta t f(y_k, t, \theta),$$

which mirrors the structure of residual networks (ResNet). The continuous-time perspective enables new approaches to neural network architecture design [3, 4], and facilitates efficient training via the adjoint equation, which generalises the classical backpropagation algorithm [15] to the continuous time. Schrödinger's equation is also of the form in Eq. (3), and one may utilise classical machine learning for quantum machine learning problems. However, there is a concern of the scalability in dimensionality of classical machine learning for high-dimensional quantum systems, which motivates the study in the follow-up sections.

The finite-dimensional state $y(t)$ in Eq. (3) can be generalised to a function $u(t)$, with f replaced by a parameterised differential operator \mathcal{D} , leading to what we refer to as neural PDEs:

$$\frac{d}{dt} u(t) = \mathcal{D}(u(t), t, \theta).$$

Depending on the training scheme and loss function, this approach is known by various names in the literature, such as PDE-Net [6] and physics-informed neural networks (PINN) [7], among others.

III. QUANTUM NEURAL ODE AND PDE: SCOPE AND APPLICATIONS

For *any* learning algorithm whose task is to learn an approximation of unknown quantum states (parameterised as $\rho(\theta)$) or unknown quantum channels (parameterised as $\mathcal{E}(\theta)$), it must involve a functional mapping between the quantum system to a loss value,

$$\mathcal{L} : \quad \rho(\theta), \mathcal{E}(\theta) \rightarrow \mathbb{R}, \quad \theta = (\theta_1, \dots, \theta_M) \in \mathbb{R}^M,$$

where one aims to solve for θ obeying

$$\operatorname{argmin}_\theta \mathcal{L}_\theta \quad (4)$$

where we use the notation \mathcal{L}_θ for simplicity, and it should be understood as $\mathcal{L}_\theta = \mathcal{L}(\rho(\theta))$ or $\mathcal{L}_\theta = \mathcal{L}(\mathcal{E}(\theta))$ depending on the context. Due to the close relationship between the quantum channel that creates the density matrix from a known state and the density matrix itself, without loss of generality, we will consider $\mathcal{L}_\theta = \mathcal{L}(\rho(\theta))$ mostly below.

Since all quantum states or channels ultimately arise from physical processes, they must also evolve in real, continuous time $t \in \mathbb{R}$. Any discretisation in time that arises in some scenarios – for instance in digital quantum simulation – is some approximation of the continuous time setting. The so-called discrete-time settings in reality cannot be truly discrete since quantum speed limits [29] fundamentally forbids the instantaneous application of two distinguishable quantum channels one after the other. Furthermore, we will see that there are many natural applications where continuity in time is an essential requirement. Thus, for these learning tasks, we must consider the dynamical laws – in continuous time t – corresponding to the quantum state $\rho(t, \theta)$ and quantum channels $\mathcal{E}(t, \theta)$. The corresponding loss function $\mathcal{L}_\theta(t = T)$ can either result from $\rho(t = T, \theta)$ or $\mathcal{E}(t = T, \theta)$ at some terminal time T or certain running cost e.g., $\mathcal{L}_\theta = \int_0^T \mathcal{L}(\rho(t, \theta)) dt$ or be a combination of both (for instance in general quantum optimal control problems). Since the running cost after being discretised could be viewed as a linear combination of terminal costs, we will simply consider the terminal cost throughout this work.

Given the form of \mathcal{L}_θ that is motivated by the learning problem at hand, the key next step is to approximately solve Eq. (4). One may use non-gradient based optimisation methods which have also been used in [18, 21]. For more efficiency in optimisation, we will focus on the gradient-based methods for Eq. (4). Gradient-based methods require first and foremost the efficient computation of the gradients $\partial \mathcal{L} / \partial \theta_m$, $m = 1, \dots, M$. When the system dimension is large, in some scenarios it is possible to use quantum simulation to compute the gradient more efficiently. For digital quantum devices, a widely studied approach is the parameter-shift rule [17, 32–35], which has recently also been used in [22] to design a forward-type algorithm. It remains an open question whether a backward-type algorithm is possible, which is addressed by our new quantum algorithms in Section IV. The full details of quantum algorithms for gradient computation are given in Section IV. We will see that these gradient computation algorithms require the ability to prepare – as an initial state input – either the functional derivative $\frac{\delta \mathcal{L}}{\delta \rho} |_{\rho=\rho(T)}$ being proportional to a density matrix or require $\frac{\delta \mathcal{L}}{\delta \rho} |_{\rho=\rho(T)}$ to be expressed as a known linear combination of density matrices which can each be prepared.

Note that \mathcal{L}_θ is a functional on the space of density operators, equipped with Hilbert-Schmidt inner product, the change of the loss function, denoted as $\frac{\delta \mathcal{L}}{\delta \rho}$, is defined as follows:

$$\frac{d}{d\epsilon} \mathcal{L}(\rho + \epsilon A) \Big|_{\epsilon=0} = \operatorname{tr} \left(\frac{\delta \mathcal{L}}{\delta \rho} A \right), \quad \text{for all feasible Hermitian operators } A.$$

Note that $\frac{\delta \mathcal{L}}{\delta \rho}$ is a *Hermitian operator* on the Hilbert space of the original quantum system \mathcal{H} . An important class of loss functions that can satisfy the above conditions includes

$$\mathcal{L}_\theta = \operatorname{tr}(\rho(T, \theta) O), \quad O = \sum_{j=1}^J c_j O_j = O^\dagger, \quad O_j^\dagger = O_j \succeq 0, \quad \operatorname{tr}(O_j) = 1, \quad c_j \in \mathbb{R}, \quad (5)$$

where $\rho(t, \theta) = \mathcal{E}(t, \theta)(\rho_0)$ can obey either closed quantum dynamics or open quantum dynamics, c_j are known constants and we assume we can be given access to r_j as density matrices. For example, here it is clear that $\frac{\delta \mathcal{L}}{\delta \rho}|_{\rho=\rho(T)} = O$. Although we will examine applications in Sections III B – III F where the loss functions can mostly be expressed in the form in Eq. (5), the formalism itself is not solely confined to this loss function form. The quantum circuits for the gradient estimation algorithms in Section (IV) can also be applied to generic loss functions.

A. Quantum neural ODEs and PDEs

To proceed with this fairly general setting, we first need to define the concept of quantum neural ODEs and PDEs, analogously to (classical) neural ODEs/PDEs, so we focus primarily the formulation where $\rho(t, \theta)$ evolves via dynamics in *continuous time*, rather than discrete time.

Definition 1. Let the unitary evolution of the initial quantum state with density matrix ρ_0 obey the dynamical equation

$$\frac{\partial \rho(t, \theta)}{\partial t} = -i[H(t, \theta), \rho(t, \theta)], \quad \rho(0, \theta) = \rho_0, \quad H(t, \theta) = H^\dagger(t, \theta), \quad \theta = (\theta_1, \dots, \theta_M). \quad (6)$$

The parameters $\{\theta_m\}_{m=1}^M$ are tuned to optimise a given loss function \mathcal{L}_θ . We refer to the system in Eq. (6) with its corresponding \mathcal{L}_θ collectively as

- (1) a (closed) *quantum neural ordinary differential equation (QNODE)*, if $\rho(t, \theta)$ are finite D -dimensional quantum states (DV);
- (2) a (closed) *quantum neural partial differential equation (QNPDE)* when $\rho(t, \theta)$ are a system of d qumodes (CV);
- (3) a (closed) *hybrid QNPDE* when $\rho(t, \theta)$ is a hybrid CV-DV quantum state.

If $\rho(t, \theta) = \mathcal{E}(t, \theta)(\rho_0)$ where $\mathcal{E}(t, \theta)$ is a quantum channel that instead describes open quantum system dynamics, then depending on if $\rho(t, \theta)$ is a DV or CV, or hybrid DV-CV quantum state, the corresponding ODE or PDE for $\rho(t, \theta)$ is referred to as an *(open) QNODE*, *(open) QNPDE* or *(open) hybrid QNPDE*.

In this paper, we examine this formalism for wide range of applications of general closed QNODEs/QNPDEs for loss functions of the type in Eq. (5). In these cases, it is sufficient to learn the generating Hamiltonian $H(t, \theta)$ in Eq. (6), which has the general decomposition

$$H(t, \theta) = \sum_{k=1}^K f_k(t, \theta) H_k, \quad f_k(t, \theta) \in \mathbb{R}, \quad H_k = H_k^\dagger, \quad (7)$$

where H_k are time-independent Hermitian operators and $H_k \neq H_{k'}$ for all $k \neq k'$. If classical data $z \in \mathbb{R}^N$ is also included, then we can augment $H(t, \theta) \rightarrow H(t, \theta, z) = \sum_{k=1}^K f_k(t, \theta, z) H_k$, but we will suppress the z parameters for simplicity unless explicitly required.

For finite D -dimensional quantum systems, if the Lie algebra generated by the set $\{iH_k\}_{k=1}^K$ under commutation and linear combination is dense in $SU(D)$, then $H(t, \theta)$ can generate an arbitrary unitary $U(t) = \mathcal{T} \exp(-i \int_0^t H(\tau, \theta) d\tau)$ with suitably chosen $f_k(t, \theta)$ and in general $K_{\max} = D^2 - 1$, although many terms $f_k(t, \theta)$ can also be zero and we can also have $K \ll D^2 - 1$ depending on applications that do not require universality. Below are a few examples of Eq. 7. When $D = 2$, $H_1 = \sigma_x, H_2 = \sigma_y, H_3 = \sigma_z$. For continuous-variable quantum systems, for approximate universality in generating unitaries, it is sufficient for the set $\{H_k\}_{k=1}^K$ to contain only up to quadratic Hamiltonians (i.e., degree one or two in \hat{x}, \hat{p}) that generate only Gaussian operations, and only a single non-Gaussian Hamiltonian (e.g., $H_k = \hat{x}^3$) and access to arbitrary $f_k(t)$ [36]. For example, for a single qumode, $H_1 = \hat{x}, H_2 = \hat{p}, H_3 = \hat{x}^2, H_4 = \hat{p}^2, H_5 = \hat{x} \hat{p}, H_6 = \hat{x}^3$ is one possible choice.

There are primarily two types of applications to consider and these demonstrate the two key advantages of this continuous-time formalism:

- (Special classes of data – no universality required): It naturally captures the class of learning problems where the data arises directly from continuous-time dynamics associated with Eq. (6) or with ODEs/PDEs that can be naturally mapped onto Eq. (6). This includes most scenarios that arise from physical phenomena obeying known linear dynamical laws and some obeying nonlinear dynamics. Here H_k appears naturally and K is not often too large;
- (General data – universality required): It can also capture the class of learning problems more appropriate for “messy dynamics”, where the form of the dynamical laws that naturally generates these data are not generally known nor can be written in simple form (e.g. dynamics generating pictures of cats versus those generating dogs). Then universality in representation is more appropriate, and the learning task is to approximate $f_k(t, \theta)$ using some basis expansion. Although it is sufficient to choose $K = K_{\max}$, but $K \ll K_{\max}$ is also possible by appropriate choices of $f_k(t, \theta)$, and these different choices correspond to different “learning architectures”.

Here the choices of $\{f_k(t, \theta)\}_{k=1}^K$ and the basis which we choose to approximate these functions is thus a central question. The form of $f_k(t, \theta)$ could arise from either (not deliberate) natural dynamics, or it could arise from (deliberate) quantum control. In quantum control $H(t, \theta) = H_0 + \sum_{k=1}^K f_k(t, \theta)H_k$ where H_0 is the drift (free) Hamiltonian and $\sum_{k=1}^K f_k(t, \theta)H_k$ is known as the control Hamiltonian and $f_k(t, \theta)$ are the time-dependent control functions. One key class of control fields is chirped fields, which dynamically modulates frequencies to achieve precise quantum state transitions. For example (1) $f_k(t, \theta) = \sum_i f_k^{(i)}(\theta)(\Theta(t - t_i) - \Theta(t - t_{i+n_i}))$ are piecewise constant, where the time interval of each non-trivial signal is $t_{i+n_i} - t_i$. The notation Θ denotes the Heaviside function on the real line. This is known as bang-bang control and also corresponds to the gate-based circuit picture for quantum simulation; (2) $f_k(t, \theta) = \sum_n a_n^{(k)}(\theta) \cos(n\omega_k(\theta)t) + b_n^{(k)}(\theta) \sin(n\omega_k(\theta)t)$ corresponds to harmonic driving, and appears for example in NMR pulse shaping and Rabi oscillations; (3) $f_k(t, \theta) = \sum_n a_n^{(k)}(\theta) e^{-i\omega_{n,k}(\theta)t}$ for example used in GRAPE; (4) $f_k(t, \theta) = \sum_n c_n^{(k)}(\theta) t^n$ is used in higher-order optimal control; (5) $f_k(t, \theta) = \sum_n A_n^{(k)}(\theta) e^{-(t-T/2)^2/2\sigma_{n,k}^2(\theta)}$ corresponds to Gaussian or adiabatic control, and appears in Stimulated Raman adiabatic passage (STIRAP) in quantum state transfer and adiabatic quantum computing.

This formulation with simple loss functions of the form in Eq. (5) is already relevant to a broad range of applications, including:

- (1) learning an unknown quantum state preparation and Hamiltonian learning (Section III B)
- (2) certain learning problems in open quantum systems (Section III C)
- (3) learning (classical) ODEs/PDEs (Sections III D)
- (4) learning non-autonomous systems (Section III E) and
- (5) providing a general formulation for a large class of quantum neural networks (Section III F) in the continuous-time limit, from which new quantum neural network architectures could emerge from choosing different discretisations.

We will now examine each application in turn below and provide simulations for simple toy examples in Section V.

B. Learning in closed quantum systems

Quantum state preparation – The first application we can consider is quantum target state preparation from a known initial state ρ_0 . Here the task is to approximate a given state σ , where we choose the loss function as follows:

$$\mathcal{L}_\theta = 1 - \text{tr}(\sigma\rho(T, \theta)) \equiv \text{tr}((\mathbf{1} - \sigma)\rho(T, \theta)), \quad (8)$$

where $\rho(T, \theta) = U(T, \theta)\rho_0U^\dagger(T, \theta)$ and $\sigma = U\rho_0U^\dagger$ and U may be a black-box. This is a relevant loss function whether ρ_0 is a pure or a mixed state. When ρ_0 is a pure state, then the loss function is simply

$1 - F(\rho(T, \theta), \sigma)$ where $F(\rho(T, \theta), \sigma)$ is the quantum fidelity between σ and $\rho(T, \theta)$. When ρ_0 is a mixed state, then minimising the above loss function is equivalent to minimising the Hilbert-Schmidt norm of quantum states, since

$$\begin{aligned} \operatorname{argmin}_{\theta} \frac{1}{2} \|\rho(T, \theta) - \sigma\|_{\text{HS}}^2 &= \operatorname{argmin}_{\theta} \frac{1}{2} \operatorname{tr}((\rho(T, \theta) - \sigma)^2) \\ &= \operatorname{argmin}_{\theta} \frac{1}{2} \left(\operatorname{tr}(\rho(T, \theta)^2) + \operatorname{tr}(\sigma^2) \right) - \operatorname{tr}(\sigma \rho(T, \theta)) \\ &= \operatorname{argmin}_{\theta} \operatorname{tr}(\rho_0^2) - \operatorname{tr}(\sigma \rho(T, \theta)) \\ &= \operatorname{argmin}_{\theta} \mathcal{L}_{\theta}, \end{aligned}$$

where $\|\cdot\|_{\text{HS}}$ denotes the Hilbert-Schmidt norm and the purity of $\rho(T, \theta)$ does not change under unitary transformation $U(T, \theta)$ so $\operatorname{tr}(\rho^2(T, \theta)) = \operatorname{tr}(\rho_0^2)$ and similarly applies to $\sigma = U \rho_0 U^\dagger$. For simulations of a toy example, see Section [V A](#).

We note that this differs from the canonical target state preparation, since we assume the classical description of the target state is not provided. Although the target is a quantum state that cannot be cloned, we assume access to trusted copies of a pure quantum state $\frac{\delta \mathcal{L}}{\delta \rho}|_{\rho=\rho(T)} \propto \sigma$ from a third party, but the state preparation procedure (i.e., the black-box quantum dynamics U) is hidden from us. Our goal is to learn this preparation. This can be viewed as a certain quantum analogue of a generative model, whose classical version aims to find a dynamics (or mapping) to reproduce a probability distribution given finite samples.

Hamiltonian-learning with access to input and output states – Suppose there is a Hamiltonian dynamics $H(t)$ and we only have access to the inputs and outputs of the corresponding unitary evolution $U(t)$, and we can control the total evolution time [24]. The goal is to find a representation of this unknown system by identifying the Hamiltonian $H(t, \theta) \sim H(t)$ that generates this unitary. Such a Hamiltonian may describe either a finite-dimensional quantum system (Hamiltonian learning for ODEs) or an infinite-dimensional (continuous-variable) quantum system (Hamiltonian learning for PDEs). Unlike the previous example, where we assumed access to a single output state σ , here we assume an oracle access to the entire unitary generated by the unknown Hamiltonian, thus allowing us to use different input states and possibly different evolution time.

To probe the system, we prepare a set of initial (pure) states $\{\rho_j\}_{j=1}^{M_s}$, which are input into the black box quantum system, which returns the corresponding quantum states at various times T_j , denoted as $\{\sigma_j(T_j)\}_{j=1}^{M_s}$. We can also input these initial states into a controllable and trustful unitary system generated by a parameterised Hamiltonian $H(t, \theta)$, with outputs $\{\rho_j(T_j, \theta)\}_{j=1}^{M_s}$. Our aim is to find a parameterised Hamiltonian $H(t, \theta)$ that best approximates the corresponding unitary evolution. The loss function is naturally defined as:

$$\mathcal{L}_{\theta} = \frac{1}{M_s} \sum_{j=1}^{M_s} \left(1 - \operatorname{tr}(\sigma_j(T_j) \rho_j(T_j, \theta)) \right), \quad (9)$$

which is simply a linear combination of loss functions as in Eq. (8) from the previous example. We remark that this loss function is similar to the one used in gate synthesis tasks in [22] mathematically – but their application settings are different. This approach has a similar flavor as the interactive quantum likelihood evaluation (IQLE) in [24]. For a numerical example, see Section [V](#).

Hamiltonian-learning with access to observables of output operators – In this case we are still in the Hamiltonian-learning framework as in the previous example, except now we assume access only to the expectation values of observables, not the initial and final quantum state outputs. In this case, we minimize

$$\mathcal{L}_{\theta} = \frac{1}{M_s N} \sum_{i=1}^{M_s} \sum_{j=1}^N \left| \operatorname{tr}(O_j \sigma_i(T_i)) - \operatorname{tr}(O_j \rho_i(T_i, \theta)) \right|^2, \quad (10)$$

where O_j are observables. This loss function aims to match the tomography data of the target and parameterised states [37], or, in mathematical terms, estimates the gap using the weak formalism.

For each term in the sum with observable operator O_j , fixed input state ρ_i , and time T_i (we omit subscripts below for simplicity), the functional derivative is

$$\frac{\delta \mathcal{L}}{\delta \rho} \Big|_{\rho=\rho(T,\theta)} = 2 \left(\text{tr}(O\rho(T,\theta)) - \text{tr}(O\sigma(T)) \right) O, \quad (11)$$

so $\frac{\delta \mathcal{L}}{\delta \rho} \Big|_{\rho=\rho(T,\theta)} \propto O$. When $\rho(T,\theta)$ is a finite-dimensional quantum system, then all observables $O = \sum_i c_i |i\rangle\langle i|$, $i = i_1 \cdots i_n \in \{0,1\}^{\otimes n}$ can be written in terms of weighted sums of states in the computation basis. When O are local Pauli matrices, e.g., $O = \sigma_X \otimes \mathbf{1}$, then we can decompose this as $O/2 = |+\rangle\langle +| \otimes \mathbf{1}/2 - |-\rangle\langle -| \otimes \mathbf{1}/2$, where each term corresponds to a density matrix; see also Appendix C 2 for other examples. Since $\frac{\delta \mathcal{L}}{\delta \rho} \Big|_{\rho=\rho(T,\theta)}$ above is not normalised, there is a prefactor term that affects the contribution of each gradient term when summed, and thus influences the learning rate. See a numerical example and discussion about dealing with the normalisation prefactor in Section V.

C. Learning in open quantum systems

We first examine the loss function in Eq. (5) where $\rho(t,\theta) = \mathcal{E}(t,\theta)(\rho_0)$ now undergoes open quantum dynamics. This scenario arises from the ability to probe only a sub-system of a large closed quantum system. Our goal is to find an effective closed Hamiltonian dynamics as a surrogate model for the original Hamiltonian. Hence, we parameterise the purification of $\rho(t,\theta)$ by defining a parameterised unitary $U(t,\theta)$ and a pre-determined initial ancilla state $|e\rangle\langle e|$ where $\mathcal{E}(t,\theta)(\rho_0) = \text{tr}_e(U(t,\theta)(\rho_0 \otimes |e\rangle\langle e|)U^\dagger(t,\theta))$. Thus Eq. (5) becomes

$$\mathcal{L}_\theta = \text{tr}(M R(T,\theta)), \quad M = O \otimes \mathbf{1}_e, \quad R(T,\theta) = U(T,\theta)(\rho_0 \otimes |e\rangle\langle e|)U^\dagger(T,\theta),$$

where \mathcal{L}_θ and unitary dynamics for $R(T,\theta)$ can still be described with a (closed) QNODE/QNPDE. Then the same applications in Section III B still apply here, except here we are instead learning the purification of a target state and the Hamiltonians generating the purification.

We can also look at an alternative loss function that is nonlinear in $\rho(t,\theta)$, namely one minus the purity of the state

$$\mathcal{L}_\theta = 1 - \text{tr}(\rho^2(T,\theta)), \quad \rho(T,\theta) = \text{tr}_e(U(T,\theta)(\rho_0 \otimes |e\rangle\langle e|)U^\dagger(T,\theta)). \quad (12)$$

This loss function is associated with learning the purification of $\rho(t,\theta)$ itself. Here

$$\frac{\delta \mathcal{L}}{\delta \rho} \Big|_{\rho=\rho(T)} \propto \rho(T,\theta),$$

which we assume can be prepared to serve as an input quantum state to the gradient estimation algorithms in Section IV. Another nonlinear loss function is the Rényi entropy, $\mathcal{R}_n(\rho) = \frac{1}{1-n} \ln \text{tr}(\rho^n)$, which has been used to study the entanglement [38] if ρ is a reduced density matrix as above, and the $n = 2$ case is related to purity. For $n > 3$, $\delta \mathcal{L}/\delta \rho \propto \rho^{n-1}/\text{tr}(\rho^n)$ needs to be prepared, and this could be achieved for instance through a block-encoding. We will not consider these settings in this paper.

D. Learning ODEs and PDEs

Learning (classical) ODEs and PDEs is a large application area in (classical) machine learning. Of special interest to us are cases where the size or dimension of the ODE or PDE is very large – so the gradients of the corresponding loss functions may not be classically efficient to compute, as it necessarily involves the simulation of the ODE or PDE themselves. Most classical methods, like finite-difference, finite element or spectral methods, suffer from the curse of dimensionality. In these cases, it is possible instead to leverage

quantum algorithms to simulate the corresponding ODEs and PDEs to obviate the curse of dimensionality. This could serve as an alternative approach to classical machine learning for high-dimensional PDEs [7, 39]. These quantum algorithms can then be embedded inside their corresponding QNODE, QNPDEs to employ quantum algorithms also for the gradient computation required in the learning of (classical) ODEs and PDEs.

We first focus our attention to linear ODEs and PDEs for $\mathbf{u}(t)$ of the form

$$\frac{d\mathbf{u}(t)}{dt} = -i\mathbf{A}(t)\mathbf{u}(t), \quad \mathbf{u}(t=0) = \mathbf{u}_0, \quad (13)$$

where in general $\mathbf{A}(t) \neq \mathbf{A}^\dagger(t)$. Eq. (13) denotes a system of D linear ODEs when $\mathbf{u}(t) = \sum_{i=1}^D u_i(t)|i\rangle$ is a D -dimensional quantum state and $\mathbf{A}(t)$ is a $D \times D$ matrix. Eq. (13) can also denote a $d+1$ -dimensional linear PDE when $\mathbf{u}(t) = \int u(t, x)|x\rangle dx$ is a system of d qumodes with $x \in \mathbb{R}^d$, and $\mathbf{A}(t)$ is composed of quadrature operators \hat{x}, \hat{p} using the correspondence $x \rightarrow \hat{x}, \partial/\partial x \rightarrow i\hat{p}$, see [25]. Eq. (13) can also denote a system of D linear $d+1$ -dimensional PDEs, then $\mathbf{u}(t) = \int \sum_{i=1}^D u_i(t, x)|i\rangle |x\rangle dx$ is a hybrid CV-DV quantum state.

It is possible to use the (closed) QNODE, QNPDE formalism for general *non-unitary* evolution in Eq. (13) if we can map the system in Eq. (13) in a very simple way to the system in Eq. (6), i.e., a simple correspondence between $\mathbf{A}(t)$ and $H(t)$. This can be realized by Schrödingerisation (see [25, 26] and references therein), where the corresponding system in Eq. (6) acts on a system of the same size as Eq. (13) plus one ancilla qumode. With Schrödingerization, one can recover $\mathbf{u}(t)$ from Eq. (13) by first simulating the solution $\mathbf{v}(t)$ following unitary dynamics (equivalent to Eq. (6) with the association $\rho(t) = \mathbf{v}(t)\mathbf{v}^\dagger(t)$ up to a normalisation)

$$\begin{aligned} \frac{d\mathbf{v}(t)}{dt} &= -i\mathbf{H}(t)\mathbf{v}(t), & \mathbf{H}(t) &= \mathbf{A}_2(t) \otimes \hat{\eta} + \mathbf{A}_1(t) \otimes \mathbf{1}_\eta = \mathbf{H}^\dagger(t), \\ \mathbf{v}(t=0) &= \mathbf{u}_0 \otimes |\Xi\rangle, & |\Xi\rangle &= \int e^{-|\xi|} |\xi\rangle d\xi, & \xi \in \mathbb{R} \\ \mathbf{A}_1(t) &= \frac{1}{2}(\mathbf{A}(t) + \mathbf{A}^\dagger(t)) = \mathbf{A}_1^\dagger(t), & \mathbf{A}_2(t) &= \frac{i}{2}(\mathbf{A}(t) - \mathbf{A}^\dagger(t)) = \mathbf{A}_2^\dagger(t), \end{aligned} \quad (14)$$

where $\hat{\xi}, \hat{\eta}$ are conjugate quadrature operators obeying $[\hat{\eta}, \hat{\xi}] = i\mathbf{1}_\eta$ and they have corresponding orthonormal bases $\{|\xi\rangle\}_{\xi \in \mathbb{R}}, \{|\eta\rangle\}_{\eta \in \mathbb{R}}$ with $\hat{\xi}|\xi\rangle = \xi|\xi\rangle$ and $\hat{\eta}|\eta\rangle = \eta|\eta\rangle$. Then $\mathbf{u}(t)$ can be recovered from $\mathbf{v}(t)$ by projecting the extra ancilla qumode onto the positive eigenvalues $|\xi| > 0$

$$|\mathbf{u}(t)\rangle = \frac{\mathbf{u}(t)}{\|\mathbf{u}(t)\|} \propto \text{tr}_\xi((\mathbf{1}_x \otimes \Pi_{\xi>0})\mathbf{v}(t)), \quad \Pi_{\xi>0} = \int_{\xi>0} |\xi\rangle\langle\xi| d\xi = \Pi_{\xi>0}^\dagger.$$

Suppose we want to learn a linear ODE/PDE with a known form, but with unknown parameters. Most ODEs and PDEs that arise from applications in scientific computing and engineering usually have fairly restrictive forms. This means that the universality of representation is in fact not a requirement, and one might be learning only a relatively small number of unknown parameters (for example viscosity and heat conductivity in gas dynamics). We can thus expand

$$\mathbf{A}(t, \theta) = \sum_{k=1}^K c_k(t, \theta) A_k \quad (15)$$

with the known set of operators $\{A_k\}_{k=1}^K$ that is independent of time and tuneable parameters θ . These are easily determined from the given form of ODE/PDE. The corresponding Hamiltonian in the QN-ODE/QNPDE formalism can now also parameterised as

$$\mathbf{H}(t, \theta) = \frac{1}{2} \sum_{k=1}^K c_k(t, \theta) (A_k \otimes \mathbf{1}_\eta + i A_k \otimes \hat{\eta}) + \frac{1}{2} \sum_{k=1}^K c_k^*(t, \theta) (A_k^\dagger \otimes \mathbf{1}_\eta - i A_k^\dagger \otimes \hat{\eta}). \quad (16)$$

To learn these parameters θ , suppose we are given access to values of observables of the true solution $\sigma(T) := \mathbf{u}(t=T)\mathbf{u}(t=T)^\dagger$, which takes the form $\text{tr}(O_j \sigma(T)) \equiv \text{tr}(O_j \mathbf{u}(t=T)\mathbf{u}(t=T)^\dagger)$, as well as

access to the normalisation constants $\text{tr}(\sigma(T))$. For ODEs, O_j can always be written as a weighted sum of computational basis states. In the context of learning PDEs, the observables would consist of expected moments over some finite domain, for example the second moment $\langle \hat{x}^2 \rangle_{x \in \mathcal{B}}$ where \mathcal{B} is some bounded region in space. In this case, the corresponding observable $O_j = \hat{x}^2$ acting on $x \in \mathcal{B}$ is positive semidefinite and can be normalisable. For observables like $O_j = \hat{x}$ acting on $x \in \mathcal{B}$ which is normalisable but not positive semidefinite, can be easily decomposed as a sum of Hermitian semi-positive definite observables $O_j = \hat{x}^+ - \hat{x}^-$ where $\hat{x}^\pm = \int_{\mathcal{B}^\pm} x |x\rangle \langle x| dx \geq 0$. The procedure is similar for observables dependent on the momentum operators.

As a more concrete example, suppose we have data at collocation points, e.g., $u_j = \mathbf{u}(x_j, t = T)$ for which we can write this observable data as

$$|u_j|^2 \approx \frac{1}{|\mathcal{B}_j|} \text{tr} \left(\int_{\mathcal{B}_j} |x\rangle \langle x| \sigma(T) dx \right), \quad (17)$$

where \mathcal{B}_j is a small sub-region with Lebesgue measure $|\mathcal{B}_j|$. Hence, we can choose $O_j = \frac{1}{|\mathcal{B}_j|} \int_{\mathcal{B}_j} |x\rangle \langle x| dx$. Therefore, we also know the normalisation constant,

$$\text{tr}(\sigma(T)) \approx \sum_j |\mathcal{B}_j| \cdot |u_j|^2.$$

For physical problems, e.g., when u_j represents the temperature, then u_j is naturally positive. Assume the access to the above quadratic form in Eq. (17) is then natural. We will then denote the normalised data as

$$\frac{\text{tr}(O_j \sigma(T))}{\text{tr}(\sigma(T))} = \bar{u}_j.$$

Similar to the PINN loss [7], we can write the corresponding loss function as

$$\mathcal{L}_\theta = \frac{1}{N} \sum_{j=1}^N \mathcal{L}_j(\rho(T, \theta)) := \frac{1}{N} \sum_{j=1}^N \left| \frac{\text{tr}(O_j \sigma(T))}{\text{tr}(\sigma(T))} - \text{tr}(O_j \rho(T, \theta)) \right|^2 = \frac{1}{N} \sum_{j=1}^N |\bar{u}_j - \text{tr}(O_j \rho(T, \theta))|^2, \quad (18)$$

where the reduced density matrix

$$\rho(T, \theta) = \frac{\text{tr}_\xi \left((\mathbf{1}_x \otimes \Pi_{\xi > 0}) |v(T, \theta)\rangle \langle v(T, \theta)| \right)}{\text{tr} \left((\mathbf{1}_x \otimes \Pi_{\xi > 0}) |v(T, \theta)\rangle \langle v(T, \theta)| \right)},$$

and where the normalised wave function $|v(t, \theta)\rangle = \frac{\mathbf{v}(t, \theta)}{\|\mathbf{v}(t, \theta)\|}$. We can rewrite

$$\text{tr}(O_j \rho(T, \theta)) = \frac{\text{tr} \left((O_j \otimes \mathbf{1}_\xi) (\mathbf{1}_x \otimes \Pi_{\xi > 0}) |v(T, \theta)\rangle \langle v(T, \theta)| \right)}{\text{tr} \left((\mathbf{1}_x \otimes \Pi_{\xi > 0}) |v(T, \theta)\rangle \langle v(T, \theta)| \right)} \propto \text{tr}(M_j |v(T, \theta)\rangle \langle v(T, \theta)|),$$

where $M_j = O_j \otimes \Pi_{\xi > 0} = M_j^\dagger$. Thus, the loss function \mathcal{L}_θ in Eq. (18) can be rewritten in a form similar to Eq. (5), and also corresponds to a (closed) QNODE/QNPDE. In this case, the functional derivative takes the following form

$$\begin{aligned} & \frac{\delta \mathcal{L}_j}{\delta |v(T, \theta)\rangle \langle v(T, \theta)|} \\ &= -2 \frac{\left(\bar{u}_j - \text{tr}(O_j \rho(T, \theta)) \right)}{\text{tr} \left((\mathbf{1}_x \otimes \Pi_{\xi > 0}) |v(T, \theta)\rangle \langle v(T, \theta)| \right)} \left((O_j \otimes \Pi_{\xi > 0}) - \text{tr}(O_j \rho(T, \theta)) (\mathbf{1}_x \otimes \Pi_{\xi > 0}) \right) \end{aligned}$$

Since any positive fixed constant could be absorbed into the learning rate (as will be more clear in later sections), it is sufficient to consider

$$\frac{\delta \mathcal{L}_j}{\delta |v(T, \theta)\rangle \langle v(T, \theta)|} \propto - \left(\bar{u}_j - \text{tr}(O_j \rho(T, \theta)) \right) \left((O_j \otimes \Pi_{\xi > 0}) - \text{tr}(O_j \rho(T, \theta)) (\mathbf{1}_x \otimes \Pi_{\xi > 0}) \right).$$

Note that the value \bar{u}_j comes from data and is known; $\text{tr}(O_j \rho(T, \theta))$ could be estimated from simulating Eq. (14).

Note that the loss function in \mathcal{L}_θ in Eq. (18) might resemble loss functions in classical machine learning for learning PDEs via values at different collocation points, but here we are not learning the representation of the solution directly, but rather learning the Hamiltonian that generates the solution (which is closer in spirit to finding a generative model). Once the parameters θ in $\mathbf{H}(t, \theta)$ in Eq. (16) are learned, this is easily translatable to identifying the unknown parameters in the original ODE/PDE with the corresponding $\mathbf{A}(t, \theta)$ in Eq. (15), and is a simple one-to-one direct correspondence.

This is not only useful for learning unknown parameters of known ODEs/PDEs that arise naturally in physical systems, but also potentially in machine learning itself. For instance, in both continuous normalising flows and flow matching the task is to identify the unknown parameters in the flux of a transport equation.

We can also extend these methods by using Schrödingerisation applied to more general linear ODEs/PDEs with inhomogeneous terms and higher-order time derivatives, and also to nonlinear ODEs and nonlinear Hamilton-Jacobi and nonlinear hyperbolic PDEs [25] and even ill-posed linear PDEs [40].

We emphasise that for any application where we know the form of the underlying dynamics, then the number of unknown parameters of the underlying dynamics is relatively low. Thus, we do not require a universal representation for the corresponding Hamiltonian, and the ansatz for the form of the Hamiltonian is directly related to domain knowledge and has the least number of parameters to learn. This shows the naturalness and power of the QNODE/QNPDE formalism for these problems, since ODEs and PDEs from nature are automatically continuous in time, PDEs are continuous in space and time, and this continuous form can be preserved in the learning procedure.

E. Learning non-autonomous systems

While the above applications can be generally non-autonomous (i.e., the corresponding $H(t, \theta)$ have explicit time-dependence), there is an alternative method of making this into a time-independent problem as well, using the Sambe-Howland clock formalism [30, 41–43]. We write down the formulation for unitary evolution, but this can also be applied to non-unitary evolution from Section III D.

Suppose we have an initial quantum state ρ_0 and a time-dependent Hamiltonian ansatz $H(t, \theta)$. We can turn the task of learning an unknown time-dependent Hamiltonian $H(t, \theta)$ (for any of the loss functions in Section III B, III C and III D) into learning a corresponding time-independent Hamiltonian $\bar{H}(\theta) = \hat{p}_s \otimes \mathbf{1} + H(\hat{s}, \theta)$, where $H(\hat{s}, \theta)$ is $H(t, \theta)$ with t replaced by a quadrature operator \hat{s} . If $\rho(t, \theta)$ obeys Eq. (6), then the solution $\rho(t, \theta)$ can be reproduced by evolving an augmented system $\sigma(t, \theta)$ (by including one qumode representing a clock mode) via a time-independent Hamiltonian

$$\begin{aligned} \frac{d}{dt} \sigma(t, \theta) &= -i [\bar{H}(\theta), \sigma(t, \theta)], & \sigma(0) &= G \otimes \rho_0, \\ G &= \int g(s) |s\rangle \langle s| ds, & \bar{H}(\theta) &= \hat{p}_s \otimes \mathbf{1} + H(\hat{s}, \theta). \end{aligned}$$

When $g(s) \approx \delta(s)$, one has $\rho(t, \theta) \approx \text{tr}_s(\sigma(t, \theta))$. This means that the loss functions of the form in Eq. (5) can be rewritten in the form suitable for (closed) QNODE/QNPDE

$$\text{tr}(O \rho(t, \theta)) \approx \text{tr}(O \text{tr}_s(\sigma(t, \theta))) = \text{tr}(M \sigma(t, \theta)), \quad M = O \otimes \mathbf{1}_s.$$

Thus, simulating a non-autonomous machine learning problem is, in principle, not fundamentally different from using a time-independent ansatz. The impact of the approximation $g(s) \approx \delta(s)$ has been analyzed in [30, 43] for Hamiltonian simulation. Investigating how this bias affects optimisation outcomes is an interesting direction for future work.

F. Framework for new quantum neural network architectures

The continuous-time framework for classical dynamics offers advantages in designing novel ResNet-type architectures; see, e.g., [3–5]. This is due to the fact that the continuous-time framework reduces to the canonical ResNet architecture under a particular time-discretisation (namely Euler discretisation) and would give rise to other architectures under different discretisation of the time coordinate. Despite significant progress, continuous-time analog classical algorithms remain under-explored.

We anticipate a similar approach would also apply to quantum machine learning. In quantum machine learning, most existing work instead focuses on discrete neural network architectures, leading to discrete-time quantum gates. Most of these architectures based on qubit systems are, a fact, a particular time-dependent schedule f_k to the (closed) QNODE, and similarly for (closed) QNPDE for those systems based on qumodes.

Connection of QNODE/QNPDE to quantum neural networks:

In what follows, we will first revisit and explain why many quantum neural networks are essentially (closed) QNODE and QNPDEs, where we are seeking a functions $f_k(t, z, \theta)$ using a *piecewise-in-time expansion*. It has been briefly mentioned in e.g., [20, 22], and this focus on piecewise-in-time expansion could be one reason behind why the analog approach to quantum machine learning has not been initiated much earlier.

Typically in quantum neural networks one is trying to approximate a function $g(z) \in \mathbb{R}$ for data $z \in \mathbb{R}^D$ in D -dimensional feature space which is partly or fully embedded in a quantum state $|\psi(z)\rangle$, using L layers of discrete gates $U_l(z, \theta)$

$$\begin{aligned} g(z) \approx \tilde{g}_L(z) &= \text{tr} \left(U(z, \theta) (|\psi(z)\rangle\langle\psi(z)| \otimes |0\rangle\langle 0|) U^\dagger(z, \theta) (\mathbf{1}_\psi \otimes O) \right), \\ U(z, \theta) &= \Pi_{l=1}^L U_l(z, \theta), \quad O = O^\dagger, \\ |g(z) - \tilde{g}_L(z)| &\rightarrow 0 \quad \text{as } L \rightarrow \infty. \end{aligned} \quad (19)$$

Each U_l typically involves the unitary evolution of time-independent Pauli or multi-Pauli matrices, where the rotation angle (or say the time) is the parameter to tune. In the case of a quantum classifier for binary classification, one can use $O = \sigma_z$ [44]. Since loss functions in these cases will include terms similar to

$$\frac{1}{N} \sum_{i=1}^N |g(z_i) - \tilde{g}_L(z_i)|^2,$$

for N training data, then it's clear this is of the form of a (closed) QNODE or QNPDE, where the corresponding unitary dynamics

$$\begin{aligned} U(z, \theta) &= U(T, z, \theta) = \mathcal{T} e^{-i \int_0^T H(\tau, z, \theta) d\tau} = \Pi_{l=1}^L U_l(z, \theta), \\ U_l(z, \theta) &= \mathcal{T} e^{-i \int_{t_l}^{t_{l+1}} H_l(\tau, z, \theta) d\tau}, \quad t_L = T, \end{aligned}$$

is generated by the Hamiltonian

$$H(t, z, \theta) = \sum_{l=1}^L h_l(t, z, \theta) \hat{h}_l, \quad h_l(t, z, \theta) = h_l(z, \theta) (\Theta(t - t_l) - \Theta(t - t_{l+1})), \quad (20)$$

where \hat{h}_l can be equal to some $\hat{h}_{l'}$ for $l \neq l'$, i.e., we can apply the same operation at multiple times. We can also rewrite this as a sum of hamiltonians H_k which are not equal to each other

$$H(t, z, \theta) = \sum_{k=1}^K f_k(t, z, \theta) H_k, \quad H_k \neq H_{k'}, \quad \forall k \neq k'.$$

Discussion on the complexity:

The QNODE/QNPDE formalism in fact could assist in a deeper understanding of the concerns about the complexity scaling for many quantum neural networks. Since quantum neural networks typically correspond to a piecewise-in-time expansion of the scheduling function, this means that the larger number of time intervals, the more accurate the approximation of each $f_k(t, z, \theta)$, and this translates into a larger L . For example, in many quantum neural networks, each layer $U_l(z, \theta) = e^{i\theta_l P_l} V_l$ for fixed Pauli operators P_l and fixed unitaries V_l . For certain architectures like [45], z -dependence appears in each layer, and in other cases data embedding of z is only at the beginning and does not appear at each l . Thus the total number of layers L is equivalent to the total number of tuneable parameters M .

From the analysis in Section IV D, we learn that the total cost in estimating the gradient of the loss function for (closed) QNODEs is at most $\mathcal{O}(T^2 K^2)$ (neglecting here the error scaling due to the uncertainty in quantum measurements for simplicity). Using the fairly common quantum neural network ansatz form, K is the number of local operators which is thus typically $\text{poly}(n)$ where n is the number of qubits. Since quantum neural networks typically uses the piecewise-in-time expansion for f_k , this leads to $T = \mathcal{O}(M)$, so the total cost is $\mathcal{O}(M^2)$, and this is the typical scaling that is often discussed in the quantum neural network literature. Herein, we could use a continuous-time framework to recover the complexity scaling for a discrete-time quantum neural network. As explained in Section IV D, if we use improved sampling methods, e.g., the shadow tomography, we can expect certain parameters to improve [46]. However, we note that for many physics-motivated machine learning problems, $K = \text{poly}(n)$ and $T = \mathcal{O}(1)$, which means the quantum gradient algorithm is expected to be efficient.

From this we see that the concern about the quantum neural network backpropagation scaling with respect to the number of parameters M is only a result of the particular way that U_l is defined such that $L = M$. Since here one deals with a discrete number of layers, and improvement in estimation being achieved with increasing L means one is approximating $f_k(t, z, \theta)$ with a piecewise-in-time basis, so the precision of this approximation must therefore grow with L , and hence also with M . However, for particular problems where we fix a K and we do not use the piecewise-in-time basis for estimating $f_k(t, \theta)$, then the cost of the gradient estimation scaling in M is not in a fact a concern. For general quantum machine learning problems without prior information, a fixed K may raise concern about the universality; however, this is not an intrinsic problem for physics-driven problems such as Hamiltonian learning of some many-body systems, or quantum control problems.

Thus in this continuous-time framework, we see that particular quantum neural networks are particular instances with special choices on the basis of expansion for approximating $f_k(t, z, \theta)$. In other kinds of quantum neural networks like quantum convolutional neural networks [47], for a continuous-time version we will require (open) QNODEs/QNPDEs.

Discussion on potential advantages:

Our proposed framework of quantum neural ODEs/PDEs provides a new perspective for designing quantum circuit architectures inspired by continuous-time dynamics, analogous to how classical ODEs guide ResNet design. We can design new quantum neural network architectures by considering both alternative bases for the approximation of $f_k(t, z, \theta)$, then applying different forms of discretisations in time. We will examine this in more detail in a later work.

For universal approximation in the sense of approximating an unknown function $g(z)$ (e.g. in Eq. (19)), it is currently unclear, even for classical algorithms, which architecture – ODE-based or discrete-time ResNet-based – is more efficient, as this is likely problem-dependent, as far as we know. Similarly, it is difficult to claim whether Hamiltonian dynamics-based architectures are generally more efficient than discrete-time quantum neural networks, if one's aim is universal approximation. In this context, this formulation can still serve as a mathematical tool from which one can study more general quantum neural networks and their gradient estimation algorithms, and provide an alternative viewpoint to generate new quantum architectures.

IV. GRADIENT ESTIMATION ALGORITHM FOR QNODE AND QNPDE

In this section, we will present quantum algorithms for estimating the gradient of loss function corresponding to the QNODE and QNPDE. This is a generalisation of classical backpropagation algorithm by extending to the continuous-time setting, and we use the idea of the backward adjoint equation used in classical neural ODEs [1]. We will first revisit the adjoint equation in Section IV A for the QNODE and QNPDE setting and then present our main gradient estimation algorithm in Section IV B (with time discretisation) and Section IV C (without time discretisation). The main quantum circuits for our two algorithms are summarized in the following Figure 1, and their costs will be discussed in Section IV D.

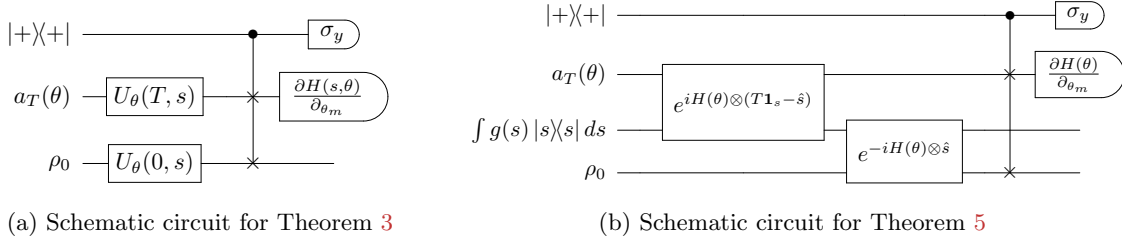


FIG. 1: The schematic quantum circuit for the gradient computation scheme with respect to parameter θ_m , $1 \leq m \leq M$. We remark that if we parameterise $H(t, \theta)$ as in Eq. (7), one does not need to perform quantum measurement for each $\frac{\partial H(s, \theta)}{\partial \theta_m}$ where $1 \leq m \leq M$; see Section IV D.

A. Revisiting the adjoint equation: application to QNODEs and QNPDEs

From Definition 1, we see that a (closed) QNODE and QNPDE evolves with the equation of motion

$$\frac{\partial \rho(t, \theta)}{\partial t} = -i[H(t, \theta), \rho(t, \theta)], \quad \rho(0, \theta) = \rho_0, \quad (21)$$

so an initial state ρ_0 evolves via unitary dynamics with respect to the unitary $U_\theta(0, t)$ where

$$\rho(t, \theta) = U_\theta(0, t)\rho_0, \quad U_\theta(0, t) = \mathcal{T} \exp(-i \int_0^t H(\tau, \theta) d\tau). \quad (22)$$

Here $\rho(t, \theta)$ is a density matrix which consists of qubits (or qumodes), and this represents a corresponding (closed) QNODE (or QNPDE) once we define a loss function \mathcal{L}_θ . Given such a loss function, we have the following lemma.

Lemma 2. *The gradient of the loss function $\mathcal{L}_\theta = \mathcal{L}(\rho(T, \theta))$ with respect to the parameter θ_m where $m = 1, \dots, M$ can be written as*

$$\frac{\partial \mathcal{L}_\theta}{\partial \theta_m} = i A_T(\theta) \int_0^T \text{tr} \left(\left[\frac{\partial H(s, \theta)}{\partial \theta_m}, a(s, \theta) \right] \rho(s, \theta) \right) ds, \quad (23)$$

when the state $\rho(s, \theta)$ evolves according to Eq. (21), and $a(s, \theta)$ evolves from a terminal condition with the same unitary dynamics as Eq. (21)

$$\begin{aligned} \frac{\partial a(s, \theta)}{\partial s} &= -i[H(s, \theta), a(s, \theta)], \\ a(T, \theta) &= a_T(\theta) = \frac{1}{A_T(\theta)} \frac{\delta \mathcal{L}}{\delta \rho} \Big|_{\rho(T, \theta)}, \quad A_T(\theta) = \text{tr} \left(\frac{\delta \mathcal{L}}{\delta \rho} \Big|_{\rho(T, \theta)} \right). \end{aligned} \quad (24)$$

Proof. This result essentially relies on the adjoint equation techniques used in e.g., classical neural ODEs [1], but here specialised to the case of unitary dynamics. We provide a customized and self-contained proof in Appendix A 1. \square

We make two remarks below:

- *Preparing the terminal state $a_T(\theta) \propto \frac{\delta \mathcal{L}}{\delta \rho}|_{\rho=\rho(T)}$:* In this formalism, we require access to the preparation of the quantum state $a_T(\theta)$. It's important to note that this is the *only* place where the form of the loss function appears. For certain loss functions, this state could be difficult to prepare. However, for many important examples that we have discussed in Section III, it is possible as the functional derivative is directly computable and has a simple form. In fact it is easy to see that $a_T(\theta)$ can also be a linear combination of quantum states that can be prepared, and the gradient in Eq. (23) is then computed as a sum of the contribution to the gradient from each of those quantum states. See Corollary 4.
- *Normalisation $A_T(\theta)$:* When we use the classical optimisation algorithms to update the parameters, then the magnitude of A_T , in fact, does not matter, as it can be absorbed into the learning rate. This also brings certain theoretical convenience: we only need to prepare the quantum state proportional to $\frac{\delta \mathcal{L}}{\delta \rho}|_{\rho=\rho(T)}$ and in this formalism, one does not need to worry about the normalisation. However, we do need to know the sign of $A_T(\theta)$, which is easily computable for many examples discussed in Section III.

B. Quantum gradient algorithm: partial time discretisation

To develop a quantum algorithm for computing the gradient of the loss function, we want to rewrite the expression in Eq. (23) in terms of quantum expectation values. Based on Lemma 2, we have the following theorem. A schematic quantum circuit is provided in Figure 1a.

Theorem 3 (Quantum gradient algorithm: partial time discretisation). *Consider the Hamiltonian dynamics of quantum state ρ_0 evolving under a parametric Hamiltonian dynamics in Eq. (21) with an accompanying loss function $\mathcal{L}_\theta = \mathcal{L}(\rho(T, \theta))$ at a terminal time T . Assume access to the quantum state $a_T(\theta) \propto \delta \mathcal{L} / \delta \rho|_{\rho=\rho(T, \theta)}$ (see Lemma 2). Then the gradient of the loss function can be estimated in terms of the time-integral of the expectation of the Hermitian operator $O_m(s, \theta)$ for arbitrary m ($1 \leq m \leq M$)*

$$\begin{aligned} \frac{\partial \mathcal{L}_\theta}{\partial \theta_m} &= 2A_T(\theta) \int_0^T \text{tr}(O_m(s, \theta) \eta(s, \theta)) \, ds, \\ O_m(s, \theta) &= \sigma_y \otimes \frac{\partial H(s, \theta)}{\partial \theta_m} \otimes \mathbf{1}, \quad m = 1, \dots, M. \end{aligned} \tag{25}$$

The quantum state $\eta(s, \theta)$ can be prepared using a unitary operation $\mathcal{V}_\theta(s)$ in the following way:

$$\begin{aligned} \eta(s, \theta) &= \mathcal{V}_\theta(s) \eta(0, \theta) \mathcal{V}_\theta(s)^\dagger, \\ \eta(0, \theta) &= |+\rangle\langle+| \otimes a_T(\theta) \otimes \rho_0, \\ \mathcal{V}_\theta(s) &:= \mathcal{C}_{\text{swap}}(\mathbf{1} \otimes U_\theta(T, s) \otimes U_\theta(0, s)), \\ \mathcal{C}_{\text{swap}} &:= |0\rangle\langle 0| \otimes \mathbf{1} \otimes \mathbf{1} + |1\rangle\langle 1| \otimes \mathbf{S}, \end{aligned} \tag{26}$$

where \mathbf{S} is the SWAP operator and $U_\theta(s, s') = \mathcal{T} \exp(-i \int_s^{s'} H(\tau, \theta) d\tau)$.

Proof. See Appendix A 2. □

To turn the above theorem into a more concrete algorithm, we can do the following:

- It is possible to compute the time integral in Eq. (25) by discretising in time, so we can choose N_t grid points s_1, s_2, \dots, s_{N_t} from $[0, T]$. Then each gradient can be computed from N_t expectation values.
- Alternatively, one may directly sample $s \in \text{Uniform}(0, T)$ which provides a stochastic approximation of the gradient, as is also used in [22].

Corollary 4. *Suppose $a_T(\theta) \propto \frac{\delta \mathcal{L}}{\delta \rho}|_{\rho=\rho(T, \theta)}$ is itself not a density matrix, but can be written as a known linear combination of density matrices $\{a_{T,j}(\theta)\}_{j=1}^J$, so $a_T(\theta) = \sum_{j=1}^J c_j a_{T,j}(\theta)$, where each $a_{T,j}(\theta)$ is proportional*

to a density matrix and $c_j \in \mathbb{R}$. This can happen for example when $\mathcal{L}_\theta = \sum_{j=1}^J c_j \mathcal{L}_{j,\theta}$; see e.g., Eq. (11) in Section III B for a concrete example. Then

$$\begin{aligned} \frac{\partial \mathcal{L}_\theta}{\partial \theta_m} &= 2 \sum_{j=1}^J c_j A_{T,j}(\theta) \int_0^T \text{tr}(O_m(s, \theta) \eta_j(s, \theta)) \, ds, \quad \eta_j(s, \theta) = \mathcal{V}_\theta(s) \eta_j(0, \theta) \mathcal{V}_\theta(s)^\dagger, \\ \eta_j(0, \theta) &= |+\rangle\langle +| \otimes a_{T,j}(\theta) \otimes \rho_0, \quad a_{T,j}(\theta) = \frac{1}{A_{T,j}(\theta)} \frac{\delta \mathcal{L}_{j,\theta}}{\delta \rho} \Big|_{\rho(T,\theta)}, \quad A_{T,j}(\theta) = \text{tr} \left(\frac{\delta \mathcal{L}_{j,\theta}}{\delta \rho} \Big|_{\rho(T,\theta)} \right). \end{aligned}$$

When the number of terms J is moderately small, one could simply estimate observables for each term and then sum them up classically. When the size of J is extremely large, SGD or mini-batch SGD are efficient tools to reduce the cost. When c_j has certain multi-scale behavior, we can further consider applying the importance sampling adaptively. Examining how more advanced sampling techniques can be employed can be highly dependent on the problem and we leave this for later work on specific applications.

It is important to emphasise that the form of the loss function \mathcal{L}_θ only appears in the initial state input of the algorithm – preparation of the state $\eta(0, \theta)$. Apart from this initial state preparation step, the algorithm is itself agnostic to the form of the loss function, and no changes to the form of the quantum circuits for the gradient estimation is necessary if the form of the loss function changes. Thus, once the quantum circuit itself is prepared and the Hamiltonian form is decided upon, then the circuit can be reused for any other loss function so long as $\eta(0, \theta)$ can be prepared as a initial input.

C. Quantum gradient algorithm: no time discretisation

While the formulation in Theorem 3 requires a discretisation of s to compute the final integral in Eq. (25), it is also possible to devise a fully analog algorithm where no such discretisation is necessary, and the gradient of the loss function with each tuneable parameter is computed with a single expectation value. To achieve this, we introduce an augmented quantum state

$$\hat{\eta}(\theta) = \int g(s) |s\rangle\langle s| \otimes \eta(s, \theta) \, ds, \quad \int g(s) \, ds = 1, \quad (27)$$

where $\int g(s) |s\rangle\langle s| \, ds$ is a normalised (continuous-variable) quantum state in $L^2(\mathbb{R})$, and $\eta(s, \theta)$ is given in Eq. (26). Ideally, we would like the density function $g(s)$ to be close to $g_{\text{top}}(s)$ which is defined as follows:

$$g_{\text{top}}(s) = \begin{cases} 1/T, & s \in [0, T]; \\ 0, & \text{otherwise.} \end{cases} \quad (28)$$

In a real physical implementation, this exact top-hat function would need to be approximated by a smooth function $g(s)$. We first look at the case where the (closed) QNODE or QNPDE is generated by a time-independent Hamiltonian $\bar{H}(\theta)$. Then we have the following theorem where the gradient of the loss function with respect to each θ_m can be estimated using a single expectation value.

Theorem 5 (Quantum gradient algorithm: fully continuous time). *Consider the Hamiltonian dynamics of quantum state ρ_0 evolving under a parametric time-independent Hamiltonian $\bar{H}(\theta)$ and an accompanying loss function $\mathcal{L}_\theta = \mathcal{L}(\rho(T, \theta))$ at a terminal time T . Assume access to the quantum state $a_T(\theta) \propto \delta \mathcal{L}_\theta / \delta \rho|_{\rho=\rho(T,\theta)}$. Then the gradient of the loss function with respect to θ_m can be estimated in terms of a single expectation value with respect to the state $\hat{\eta}(\theta)$. The density function $g(s)$ is expected to be close to the normalised top-hat function $g_{\text{top}}(s)$.*

- The gradient of the loss function \mathcal{L}_θ with respect to θ_m can also be estimated using a single expectation value with respect to the state $\hat{\eta}$. The above results easily imply that when $g(s) = g_{\text{top}}(s)$,

$$\begin{aligned} \frac{\partial \mathcal{L}_\theta}{\partial \theta_m} &= 2 A_T(\theta) T \text{tr}((\mathbf{1}_s \otimes O_m(\theta)) \hat{\eta}(\theta)), \\ O_m(\theta) &= \sigma_y \otimes \frac{\partial \bar{H}(\theta)}{\partial \theta_m} \otimes \mathbf{1}, \quad m = 1, \dots, M \end{aligned} \quad (29)$$

where the state

$$\begin{aligned}\widehat{\eta}(\theta) &= (\mathbf{1}_s \otimes \mathcal{C}_{swap}) W \left(\int g(s) |s\rangle\langle s| \otimes \eta(0, \theta) \right) W^\dagger (\mathbf{1}_s \otimes \mathcal{C}_{swap}), \\ \eta(0, \theta) &= |+\rangle\langle +| \otimes a_T(\theta) \otimes \rho_0, \\ W &= (\mathbf{1}_{\mathcal{H}_{aux}} \otimes e^{-i\bar{H}(\theta) \otimes \hat{s}} \otimes \mathbf{1}_{\mathcal{H}_{adj}}) (\mathbf{1}_{\mathcal{H}_{aux}} \otimes e^{i\bar{H}(\theta) \otimes (T\mathbf{1}_s - \hat{s})} \otimes \mathbf{1}_{\mathcal{H}}).\end{aligned}\tag{30}$$

- When $g(s) \neq g_{top}(s)$, we can estimate the gradient of the loss function to precision

$$\left| \frac{1}{2T A_T(\theta)} \frac{\partial \mathcal{L}(\rho(T))}{\partial \theta_m} - \text{tr}(\mathbf{1}_s \otimes O_m(\theta) \widehat{\eta}(\theta)) \right| \leq \|O_m(\theta)\|_\infty \|g_{top} - g\|_{TV} \tag{31}$$

where $\|O_m(\theta)\|_\infty$ is the operator norm of $O_m(\theta)$, and $\|g_{top} - g\|_{TV}$ is the total variation distance of two probability distributions g_{top} and g .

Proof. See Appendix A 3. □

It is straightforward to generalise this for time-dependent Hamiltonians $H(t, \theta)$ by employing the method described in Section III E. In this case we set the time-independent Hamiltonian $\bar{H}(\theta) = \hat{p}_s \otimes \mathbf{1} + H(\hat{s}, \theta)$ where $H(\hat{s}, \theta)$ is just $H(t, \theta)$ with the replacement $t \rightarrow \hat{s}$. Then from Section III E we see that we can recover the solution $\rho(t, \theta) \approx \text{tr}_s(\sigma(t, \theta))$ where $\sigma(t, \theta)$ evolves unitarily with respect to the time-independent Hamiltonian $\bar{H}(\theta)$. If we rewrite loss functions of the form in Eq. (5) in the form suitable for (closed) QNODE/QNPDE (that evolves with a time-independent Hamiltonian), we have

$$\text{tr}(O\rho(t, \theta)) \approx \text{tr}(O\text{tr}_s(\sigma(t, \theta))) = \text{tr}(M\sigma(t, \theta)), \quad M = O \otimes \mathbf{1}_s. \tag{32}$$

Then Theorem 5 can be directly applied with the modification of the original $a_T(\theta) \rightarrow a_T(\theta) \otimes \mathbf{1}_s$.

D. Cost for gradient estimation

We have two gradient estimation algorithms, in Theorems 3 and 5. We will discuss their complexity and the situations where our quantum algorithms could be beneficial.

Discussion on the complexity of Theorem 3:

We first consider the formalism in Theorem 3 and we assume our QNODE or QNPDE evolves via unitary evolution generated by the Hamiltonian

$$H(t, \theta) = \sum_{k=1}^K f_k(t, \theta) H_k, \quad H_k \neq H_{k'}, \quad \forall k \neq k'.$$

Then we can estimate the gradient using a discretisation in time to estimate the integration over time $s \in [0, T]$

$$\begin{aligned}\frac{\partial \mathcal{L}_\theta}{\partial \theta_m} &\propto \int_0^T \text{tr} \left((\sigma_Y \otimes \sum_{k=1}^K \frac{\partial f_k(t, \theta)}{\partial \theta_m} H_k \otimes \mathbf{1}) \eta(s, \theta) \right) ds \\ &\approx \sum_{j=1}^{N_t} \sum_{k=1}^K \Delta s_j \text{tr} \left((\sigma_Y \otimes \frac{\partial f_k(s_j, \theta)}{\partial \theta_m} H_k \otimes \mathbf{1}) \eta(s_j, \theta) \right) \\ &= \sum_{j=1}^{N_t} \sum_{k=1}^K \Delta s_j \frac{\partial f_k(s_j, \theta)}{\partial \theta_m} \text{tr}(\sigma_Y \otimes H_k \otimes \mathbf{1} \eta(s_j, \theta)),\end{aligned}\tag{33}$$

where we have discretised the time at grid points s_1, s_2, \dots, s_{N_t} and Δs_j is the weight from the quadrature scheme. Now each of the $N_t K$ terms $\partial f_k(s_j, \theta)/\partial \theta_m$ can be computed using purely classical processing, so

this does incur any cost for the quantum simulator. Thus, even if there are M different tuneable parameters, we only need quantum algorithms to compute $\mathcal{O}(N_t K)$ different expectation values $\text{tr}(\sigma_Y \otimes H_k \otimes \mathbf{1} \otimes \eta(s_j, \theta))$ with possible repetitive measurements.

Proposition 6 (Informal statement of Proposition 10 in Appendix B). *Ignoring the cost for the state preparation of $\eta(s, \theta)$, then using the most naive recovery of expectation values, to estimate all partial derivatives $\partial \mathcal{L}_\theta / \partial \theta_m$ ($m = 1, 2, \dots, M$) within error tolerance δ with probability at least $1 - \varepsilon$, we at most require a total of*

$$\max \left\{ \mathcal{O}(T^2 K^2 \delta^{-2} \log(\frac{M}{\varepsilon})), \mathcal{O}(T^{3/2} K^{5/2} \delta^{-1/2}) \right\},$$

measurements. In general, the first term will typically dominate, so that the dominating term is typically

$$\mathcal{O}(T^2 K^2 \delta^{-2} \log(\frac{M}{\varepsilon})). \quad (34)$$

Proof. A rigorous probabilistic statement could be found in Proposition 10 in Appendix B, as well as the proof of the proposition. \square

To estimate each observable $\text{tr}(\sigma_Y \otimes H_k \otimes \mathbf{1} \otimes \eta(s_j, \theta))$ to precision δ requires at most $\mathcal{O}(\delta^{-2})$ measurements for the naive sampling cost. To the best of our knowledge, no previous literature has rigorously proved the complexity scaling in quantum gradient estimation for continuous-time quantum processes.

Note that this scaling can be improved if cleverer measurement schemes are applied, for instance in using shadow tomography [48, 49] and related methods. Using these methods, the estimation of K expectation values would only require $\log(K)$ measurements, thus, in principle, we can expect an improvement over the scaling of K .

The above scaling reveals the potential efficacy of quantum neural ODEs/PDEs, at least for certain families of quantum machine learning problems. It's important to note that this cost, no matter which measurement schemes are used, actually *does not* a priori depend on the total number of tuneable parameters θ_m , $m \in \{1, 2, \dots, M\}$ (or at most logarithmic dependence of M , which is generally unessential). In terms of state preparation for $\eta(s, \theta)$, this depends on the QNODE and QNPDE given: the analog quantum simulation, the unitary gates $U_\theta(s, s')$ and the controlled-SWAP operator. It is possible to design the analog quantum simulation for the problem at hand, for instance the simulation of specific ODEs/PDEs in Section III D, for example see [25, 50]. Even if we resort to using digital quantum simulation, it is already clear that for all cases when the digital quantum simulation of $U_\theta(s, s')$ is advantageous over the classical simulation of $U_\theta(s, s')$ – this is the very backbone of almost all effort in quantum simulation as a field – the quantum algorithm for gradient estimation will be more efficient than its classical counterpart.

We can already note a few cases where our proposed QNODE/QNPDE could be beneficial, and leave a more systemic study for future work on more specialised applications

- It is interesting to note that this formulation seems to be very suitable for learning the time-dependence of Hamiltonians for some small K and moderately small T , since the quantum resource cost does not depend on the complexity of the parameterisation of each $f_k(t, \theta)$. This is applicable for example in the learning of non-autonomous ODEs/PDEs.
- If the Hamiltonian model is the quantum Ising-type model, then $K \sim \text{poly}(n)$ where n is the number of qubits. This scaling is desirable when learning a large-scale quantum system (e.g., $n \sim 10^2$) using our algorithm, compared with machine learning using classical computers. For the short-time Hamiltonian learning problem $T = \mathcal{O}(1)$, the above scaling is polynomial with respect to the total number of qubits $\mathcal{O}(\text{poly}(n))$, which suggests that the gradient estimate could be effective.

Although this is a heuristic discussion, it already outlines the promising scaling of our approach and a more comprehensive mathematical analysis will be left for a later work.

Discussion on the complexity of Theorem 5:

In using the fully continuous-time algorithm in Theorem 5, we do not need to discretise in time at all. In that case, we only need to consider the sum of K different expectation values. Thus, not including the cost of $\hat{\eta}(\theta)$ preparation (the cost here is not significantly different from the cost in preparing $\eta(s, \theta)$ except with the addition of a qumode), we only need, in the naive case $\mathcal{O}(K\delta^{-2})$ measurements, and this can in principle be improved to $\mathcal{O}(\log(K)\delta^{-2})$ with shadow tomography. We ignore the possible quadratic improvements in δ , which usually would require the more involved procedure of amplitude amplification. For non-universal Hamiltonians, this K can be very small.

In principle, even for “near universal” Hamiltonians, K may not need to be very large, but $f_k(t, \theta)$ would need to be “high frequency” in time, since we would be rapidly alternating between the application of different Hamiltonians in time, for instance in a similar setting as quantum approximate optimisation algorithm (QAOA), where we alternate between the application of the cost and the mixer Hamiltonians [51]. The questions here are more related to the design of quantum neural networks and we leave this for future work on the relevance of QNODE and QNPDEs for the design of these networks.

We note that while these algorithms can offer up to exponential cost efficiency by delegating the relevant classical dynamics simulation to the corresponding quantum dynamics simulation and simulating this on a quantum device (especially useful for very high-dimensional problems), we do need to prepare many copies of either $\eta(s, \theta)$ using the algorithm in Theorem 3. This is purely due to the quantum non-cloning theorem. We need to prepare $\eta(s, \theta)$ for each $s = s_1, \dots, s_{N_t}$ using at least N_t copies of $\eta(s, \theta)$ since we cannot keep $\eta(s, \theta)$ while also using it to create $\eta(s' > s, \theta)$. On the other hand, by using the algorithm in Theorem 5, we do not have the same quantum non-cloning theorem issue and we just need to prepare a time-independent state $\hat{\eta}(\theta)$. However, this algorithm requires a continuous-variable treatment of the extra s -mode and it remains to be seen what kinds of implementations are possible in this setting.

V. NUMERICAL EXAMPLES

We have presented several types of loss functions suitable for Hamiltonian learning in Section III B, and in this section, we will provide numerical demonstrations and validations. We mainly consider the following examples: (a) the hydrogen molecule; (b) the quantum Ising model. The Hamiltonians for these two examples are described in Appendix C 1. Details of the training hyper-parameters can be found in Appendix C 3. Note that here we provide simulation results using Theorem 3. At this moment, we haven’t done the same thing for Theorem 5 since we do not currently have a fully continuous-time general purpose emulation device particularly for learning ODEs and PDEs. Demonstrations using Theorem 5 on fully analog quantum devices is left to future work. All results reported below are based on classical emulation using PennyLane. In the following, we consider the noise from quantum measurements to better reflect the practice; “shots” means the number of quantum measurements performed each time; “shots = inf” means exact quantum measurements without fluctuation. Since we will use very small batch, we will report the test error, namely the error measured by the fidelity between the exact quantum state and the approximated quantum state; for Hamiltonian learning problems, the reported error has been averaged over different random initial states; see Eq. (C4) in Appendix C 3 for full details.

A. State-preparation learning

A key example is quantum target state preparation for a state σ , where we choose the loss function as follows:

$$\mathcal{L}(\rho(T, \theta)) = 1 - \text{tr}(\sigma \rho(T, \theta)) \equiv \text{tr}((\mathbf{1} - \sigma)\rho(T, \theta)).$$

See also Section III B. To demonstrate Theorem 3, we consider a toy example: a single qubit with target state $\sigma = |+\rangle\langle +| = a_T(\theta)$, and it is easy to see that $A_T(\theta) = -1$. We begin with $\rho_0 = |0\rangle\langle 0|$, and use

the following ansatz: $H(\theta) = \theta_1\sigma_X + \theta_2\sigma_Y + \theta_3\sigma_Z$, and set the time period $T = 1$. The time integral is discretised using the trapezoidal rule with $\Delta s = 0.1$, and we take different numbers of shots to estimate the observable for each s . One feasible solution is $\theta^* = [0, \pi/4, 0]$, corresponding to a Pauli-Y rotation, and we compare the optimised θ to this value θ^* . Although the solution is not unique (due to the periodicity in θ_2), we initialize $\theta = [0, 0, 0]$ so that this θ^* is the closest global minimizer. As shown in Figure 2, even with a few shots, the error decays exponentially with respect to the training step in the early stage. When θ is close to θ^* , quantum measurement noise prevents further improvement in accuracy, as expected. With precise quantum measurement (see the black curve), the error consistently exponentially decays to zero, demonstrating good convergence for this example using our loss function and quantum algorithm. This example clearly demonstrates the feasibility and promise of our approach.

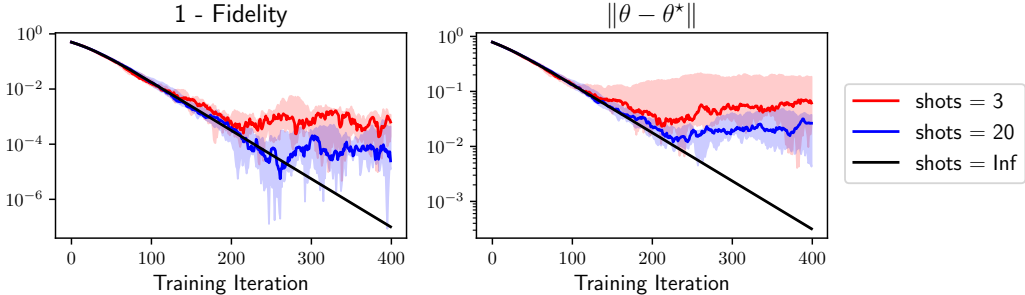


FIG. 2: The error $1 - |\langle +|U(T, \theta)|0 \rangle|^2$ versus training iterations for different numbers of shots. Shots refer to the number of repeated measurements to estimate the observables for each s in Theorem 3. Each curve represents the median error from five independent experiments; the shaded region (with the same color) indicates the corresponding minimum and maximum error during training. For the case of exact quantum measurement (black curve), there is no fluctuation in optimisation.

B. Hamiltonian learning using black-box access to the dynamics

This problem was discussed in Section III B. Its goal is to learn the unknown parameters of a Hamiltonian when we are only given the known input and output states of the dynamics generated by this Hamiltonian. To probe the system, we prepare a set of initial pure states $\{\rho_j\}_{j=1}^{M_s}$ at time zero, which are inputs into the black box. The black-box system returns the corresponding quantum states at various times T_j , denoted as $\{\sigma_j(T_j)\}_{j=1}^{M_s}$. We can also input these states into a unitary system generated by a parameterised Hamiltonian $H(t, \theta)$, with outputs $\{\rho_j(T_j, \theta)\}_{j=1}^{M_s}$. Our aim is to find a parameterised Hamiltonian $H(t, \theta)$ that best approximates the corresponding black-box unitary evolution. The loss function is naturally defined as in Eq. (9), which is also copied here $\mathcal{L}_\theta = \frac{1}{M_s} \sum_{j=1}^{M_s} \left(1 - \text{tr}(\sigma_j(T_j) \rho_j(T_j, \theta)) \right)$.

Simulation results for time-independent cases are shown in Figure 3. We use the trapezoidal rule to discretise the time integral and take different numbers of shots to estimate the observable for each s , obtaining the gradient estimate in Eq. (25). During training, we use only one sample ρ_i per parameter update, so each iteration reduces to a single unknown state learning task as in Section V A. This explains the noisy fluctuations in optimisation, even for infinite shots (i.e., exact quantum measurements) in the black curve. For the hydrogen molecule and Ising model Hamiltonians, the training is very stable even when using one sample per parameter update, as long as quantum measurement accuracy is sufficient. Even with only 10 shots per quantum estimate, the loss error decays to around 10^{-3} in terms of fidelity measurements. Notably, as the number of sites in the quantum Ising model increases, the decay rate of the loss remains nearly unchanged, even for larger systems, provided that one is given precise quantum measurements. With noisy quantum estimate, the training performance is only slightly worsen as the dimension increases. This indicates that the training problem remains efficient for relatively high-dimensional quantum systems, provided that trustful and certified quantum hardware is available.

Moreover, we have considered learning a time-dependent Ising model whose Hamiltonian and model parameterization are explained in Appendix C 1. We consider a two-site model for simplicity and the training results are visualized in Figure 4. The result is overall similar to the time-independent case. We also show a typical training result for the time-schedule in Figure 4 to validate nice accuracy of the training using our gradient estimates.

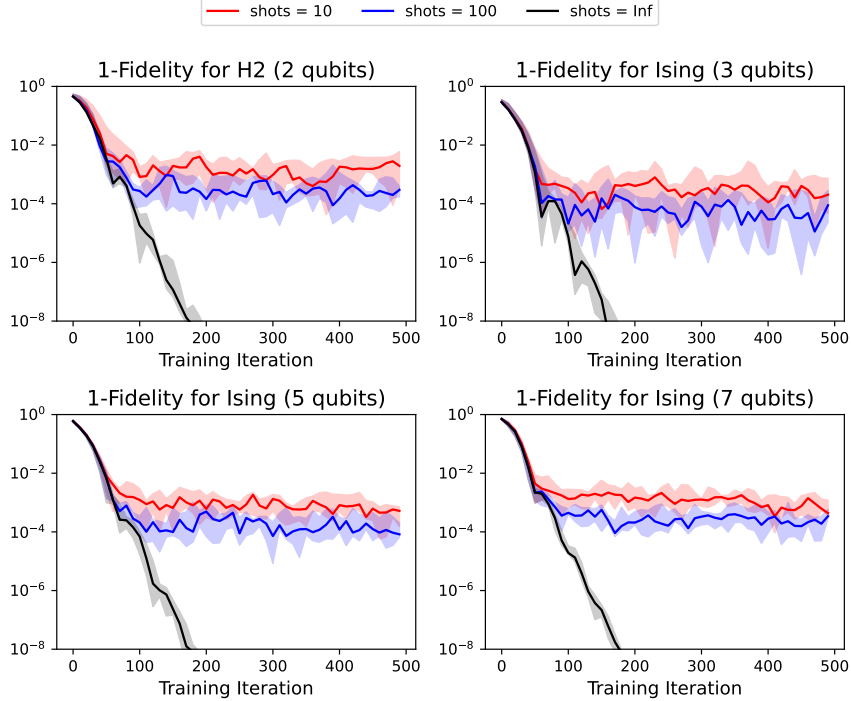


FIG. 3: Training results for Section V B for different time-independent Hamiltonians using the loss function in Eq. (9). Each curve represents the median error from five independent training runs, and the shaded region indicates the maximum and minimum error. The y-axis range is truncated for better visualization.

C. Hamiltonian learning using access to observables of an unknown quantum system

We consider the same Hamiltonian learning problem as in Section V B, except now we assume access only to the expectation values of observables, not the final quantum state outputs. This is also discussed in Section III B. In this case, we minimize

$$\frac{1}{MN} \sum_{i=1}^M \sum_{j=1}^N |\text{tr}(O_j \sigma_i(T_i)) - \text{tr}(O_j \rho_i(T_i, \theta))|^2,$$

where O_j are observables. We consider the same examples as in Section V B, except we use observable data for Eq. (10), which is also listed above for convenience. Due to the relatively higher cost of classically emulating mixed states, we consider smaller systems for this example. However, for quantum analog machines, evolving a mixed state is not fundamentally different from evolving a pure state, which brings potential advantages to run our algorithm directly on quantum devices. For each parameter update, we randomly choose one-site observables $\{\sigma_{X,Y,Z}^{(k)}\}_{k=1}^n$ (where n is the number of qubits), initialize the state at $|+\rangle\langle+|^{\otimes n}$ followed by random rotations using Rotation-(X,Y,Z), and also pick a random time T_i . These random initial sampling of input state ρ_i and T_i can help break the symmetry and overcome the appearance of new local minima

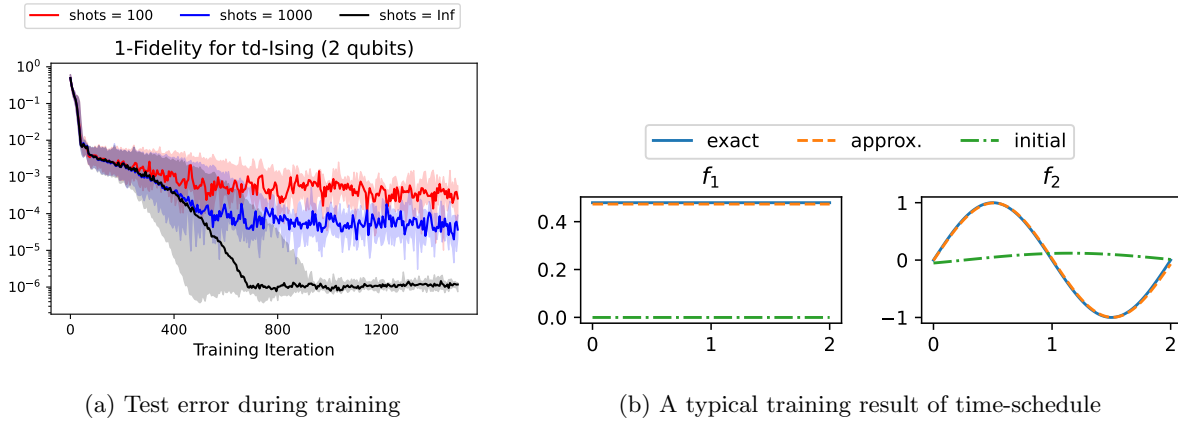


FIG. 4: Training results for Section V B for two-site time-dependent quantum Ising chain (td-Ising) using the loss function in Eq. (9). (a) Each curve represents the median error from five independent training runs, and the shaded region indicates the maximum and minimum error. (b) We show a typical training result of time-schedule using 10^3 shots per quantum estimate.

when using tomography data as the loss function in Eq. (10). Therefore, there is stochastic fluctuation in the datasets (ρ_i, T_i) , as well as in the random selection of observables. Simulation results are shown in Figure 5a, demonstrating the effectiveness and efficiency of our approach. Although the loss function in Eq. (10) is effective, we empirically note that, using tomography data as the loss function appears slightly harder to train than using an unknown state.

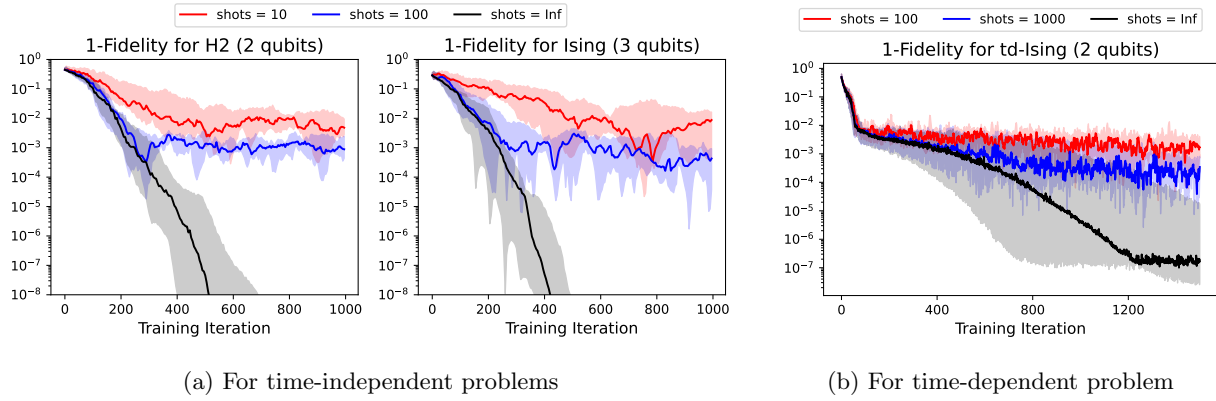


FIG. 5: Training results for Section V C using the loss function in Eq. (10): (a) for different time-independent Hamiltonians; (b) for two-site time-dependent quantum Ising chain (td-Ising). Each curve represents the median error from five independent training runs, and the shaded region indicates the maximum and minimum error.

VI. SUMMARY AND OUTLOOK

The QNODE and QNPDE framework is applicable for two classes of problems: ones where a universal Hamiltonian is not required, and one where it is required. In the former case – when the dynamics that needs to be learned can naturally be mapped onto a corresponding Hamiltonian – QNODEs and QNPDEs are particularly suitable and allow for better problem-inspired ansatzes. These applications include learning problems in both closed and some open quantum systems, learning of (classical) ODEs and PDEs, in both

autonomous and and non-autonomous settings. In the latter case – when the learning involves data generated from dynamics too complicated for simple forms and therefore a universal representation is needed – then the QNODE and QNPDE can serve as a mathematical framework that can recover existing models for quantum neural networks (which are discrete time models).

We introduce two quantum algorithms for gradient estimation for QNODEs and QNPDEs: one based on partial time discretisation and another that operates entirely in continuous time. These algorithms generalise backpropagation to the quantum regime and support a wide range of applications. For problems that do not require universal Hamiltonians, these gradient estimation algorithms can be very efficient and the costs do not a priori depend on the number of unknown parameters to be learned. Each of these applications requires more in-depth study in their own right for specific scenarios, and we leave this to future work.

Looking forward, QNODEs and QNPDEs provide a powerful lens through which quantum machine learning models can be viewed or constructed, especially in contexts where physical dynamics are naturally continuous. Beyond efficiency gains in gradient estimation, this framework opens the door to systematic architectural design inspired by physical control theory and could catalyse the development of continuous-depth quantum models. Future works will explore rigorous complexity bounds, hardware implementations, and applications to real-world quantum control and generative modeling tasks and extensions to open QNODEs/QNPDEs.

ACKNOWLEDGEMENTS

The authors would like to thank Lei Wang (Chinese Academy of Sciences) for helpful discussions. The authors acknowledge funding from the Science and Technology Commission of Shanghai Municipality (STCSM) grant no. 24LZ1401200 (21JC1402900), the NSFC grant No. 12341104, the Shanghai Jiao Tong University 2030 Initiative, and the Fundamental Research Funds for the Central Universities. YC is supported by NSFC grant No. 12401573 and is sponsored by Shanghai Pujiang Program (23PJ1404600). SJ was also partially supported by the NSFC grant No. 12426637. NL is in addition supported by grant NSFC No. 12471411.

[1] Ricky T. Q. Chen, Yulia Rubanova, Jesse Bettencourt, and David K Duvenaud, “Neural ordinary differential equations,” in *Advances in Neural Information Processing Systems*, Vol. 31 (Curran Associates, Inc., 2018).

[2] Weinan E, “A Proposal on Machine Learning via Dynamical Systems,” *Communications in Mathematics and Statistics* **5**, 1–11 (2017).

[3] Yiping Lu, Aoxiao Zhong, Quanzheng Li, and Bin Dong, “Beyond Finite Layer Neural Networks: Bridging Deep Architectures and Numerical Differential Equations,” in *Proceedings of the 35th International Conference on Machine Learning* (PMLR, 2018) pp. 3276–3285.

[4] Eldad Haber and Lars Ruthotto, “Stable architectures for deep neural networks,” *Inverse Problems* **34**, 014004 (2017).

[5] Lars Ruthotto and Eldad Haber, “Deep Neural Networks Motivated by Partial Differential Equations,” *Journal of Mathematical Imaging and Vision* **62**, 352–364 (2020).

[6] Zichao Long, Yiping Lu, Xianzhong Ma, and Bin Dong, “PDE-Net: Learning PDEs from Data,” in *Proceedings of the 35th International Conference on Machine Learning* (PMLR, 2018) pp. 3208–3216.

[7] M. Raissi, P. Perdikaris, and G. E. Karniadakis, “Physics-informed neural networks: A deep learning framework for solving forward and inverse problems involving nonlinear partial differential equations,” *Journal of Computational Physics* **378**, 686–707 (2019).

[8] Xuanqing Liu, Tesi Xiao, Si Si, Qin Cao, Sanjiv Kumar, and Cho-Jui Hsieh, “Neural SDE: Stabilizing Neural ODE Networks with Stochastic Noise,” (2019), arXiv:1906.02355.

[9] Belinda Tzen and Maxim Raginsky, “Neural Stochastic Differential Equations: Deep Latent Gaussian Models in the Diffusion Limit,” (2019), arXiv:1905.09883.

[10] Xuechen Li, Ting-Kam Leonard Wong, Ricky T. Q. Chen, and David Duvenaud, “Scalable Gradients for Stochastic Differential Equations,” in *Proceedings of the Twenty Third International Conference on Artificial Intelligence and Statistics* (PMLR, 2020) pp. 3870–3882.

[11] Patrick Kidger, James Foster, Xuechen Li, and Terry J. Lyons, “Neural SDEs as Infinite-Dimensional GANs,” in *Proceedings of the 38th International Conference on Machine Learning* (PMLR, 2021) pp. 5453–5463.

- [12] Yang Song, Jascha Sohl-Dickstein, Diederik P. Kingma, Abhishek Kumar, Stefano Ermon, and Ben Poole, “Score-Based Generative Modeling through Stochastic Differential Equations,” in *International Conference on Learning Representations* (2021).
- [13] Yang Song and Stefano Ermon, “Generative Modeling by Estimating Gradients of the Data Distribution,” in *Advances in Neural Information Processing Systems*, Vol. 32 (Curran Associates, Inc., 2019).
- [14] Jonathan Ho, Ajay Jain, and Pieter Abbeel, “Denoising Diffusion Probabilistic Models,” in *Advances in Neural Information Processing Systems*, Vol. 33 (2020) pp. 6840–6851.
- [15] David E. Rumelhart, Geoffrey E. Hinton, and Ronald J. Williams, “Learning representations by back-propagating errors,” *Nature* **323**, 533–536 (1986).
- [16] Richard P. Feynman, “Simulating physics with computers,” *International Journal of Theoretical Physics* **21**, 467–488 (1982).
- [17] Jun Li, Xiaodong Yang, Xinhua Peng, and Chang-Pu Sun, “Hybrid Quantum-Classical Approach to Quantum Optimal Control,” *Physical Review Letters* **118**, 150503 (2017).
- [18] Jirawat Tangpanitanon, Supanut Thanasilp, Ninnat Dangniam, Marc-Antoine Lemonde, and Dimitris G. Angelakis, “Expressibility and trainability of parametrized analog quantum systems for machine learning applications,” *Physical Review Research* **2**, 043364 (2020).
- [19] Danijela Marković and Julie Grollier, “Quantum neuromorphic computing,” *Applied Physics Letters* **117**, 150501 (2020).
- [20] Alicia B. Magann, Christian Arenz, Matthew D. Grace, Tak-San Ho, Robert L. Kosut, Jarrod R. McClean, Hershel A. Rabitz, and Mohan Sarovar, “From Pulses to Circuits and Back Again: A Quantum Optimal Control Perspective on Variational Quantum Algorithms,” *PRX Quantum* **2**, 010101 (2021).
- [21] Zhiding Liang, Hanrui Wang, Jinglei Cheng, Yongshan Ding, Hang Ren, Zhengqi Gao, Zhirui Hu, Duane S. Boning, Xuehai Qian, Song Han, Weiwén Jiang, and Yiyu Shi, “Variational quantum pulse learning,” in *2022 IEEE International Conference on Quantum Computing and Engineering (QCE)* (2022) pp. 556–565.
- [22] Jiaqi Leng, Yuxiang Peng, Yi-Ling Qiao, Ming Lin, and Xiaodi Wu, “Differentiable analog quantum computing for optimization and control,” in *Advances in Neural Information Processing Systems* (2022).
- [23] Araiza Bravo Oscar Rodrigo, *Analog Quantum Machine Learning Models on Near-Term Devices*, Ph.D. thesis (2024).
- [24] Nathan Wiebe, Christopher Granade, Christopher Ferrie, and D. G. Cory, “Hamiltonian learning and certification using quantum resources,” *Phys. Rev. Lett.* **112**, 190501 (2014).
- [25] Shi Jin and Nana Liu, “Analog quantum simulation of partial differential equations,” *Quantum Science and Technology* **9**, 035047 (2024).
- [26] Shi Jin, Nana Liu, and Yue Yu, “Quantum Simulation of Partial Differential Equations via Schrödingerization,” *Physical Review Letters* **133**, 230602 (2024).
- [27] Shi Jin and Nana Liu, “Quantum algorithms for nonlinear partial differential equations,” *Bulletin Math. Sci.* **194**, 103457 (2024).
- [28] Ilon Joseph, “Koopman–von neumann approach to quantum simulation of nonlinear classical dynamics,” *Physical Review Research* **2**, 043102 (2020).
- [29] A. del Campo, I. L. Egusquiza, M. B. Plenio, and S. F. Huelga, “Quantum Speed Limits in Open System Dynamics,” *Physical Review Letters* **110**, 050403 (2013).
- [30] Yu Cao, Shi Jin, and Nana Liu, “A unifying framework for quantum simulation algorithms for time-dependent hamiltonian dynamics,” arXiv preprint arXiv:2411.03180 (2024).
- [31] Aidan N Gomez, Mengye Ren, Raquel Urtasun, and Roger B Grosse, “The reversible residual network: Back-propagation without storing activations,” *Advances in neural information processing systems* **30** (2017).
- [32] K. Mitarei, M. Negoro, M. Kitagawa, and K. Fujii, “Quantum circuit learning,” *Physical Review A* **98**, 032309 (2018).
- [33] Maria Schuld, Ville Bergholm, Christian Gogolin, Josh Izaac, and Nathan Killoran, “Evaluating analytic gradients on quantum hardware,” *Phys. Rev. A* **99**, 032331 (2019).
- [34] Korbinian Kottmann and Nathan Killoran, “Evaluating analytic gradients of pulse programs on quantum computers,” (2023), arXiv:2309.16756.
- [35] David Wierichs, Josh Izaac, Cody Wang, and Cedric Yen-Yu Lin, “General parameter-shift rules for quantum gradients,” *Quantum* **6**, 677 (2022).
- [36] Seth Lloyd and Samuel L. Braunstein, “Quantum Computation over Continuous Variables,” *Physical Review Letters* **82**, 1784–1787 (1999).
- [37] Ryan O’Donnell and John Wright, “Efficient quantum tomography,” in *Proceedings of the forty-eighth annual ACM symposium on Theory of Computing*, STOC ’16 (New York, NY, USA, 2016) pp. 899–912.
- [38] Zhaoyou Wang and Emily J. Davis, “Calculating Rényi entropies with neural autoregressive quantum states,” *Physical Review A* **102**, 062413 (2020).
- [39] Weinan E and Bing Yu, “The Deep Ritz Method: A Deep Learning-Based Numerical Algorithm for Solving Variational Problems,” *Communications in Mathematics and Statistics* **6**, 1–12 (2018).

[40] Shi Jin, Nana Liu, and Chuwen Ma, “Schrödingerisation based computationally stable algorithms for ill-posed problems in partial differential equations,” arXiv preprint arXiv:2403.19123 (2024).

[41] Hideo Sambe, “Steady States and Quasienergies of a Quantum-Mechanical System in an Oscillating Field,” *Physical Review A* **7**, 2203–2213 (1973).

[42] James S. Howland, “Stationary scattering theory for time-dependent Hamiltonians,” *Mathematische Annalen* **207**, 315–335 (1974).

[43] Yu Cao, Shi Jin, and Nana Liu, “Quantum simulation for time-dependent Hamiltonians—with applications to non-autonomous ordinary and partial differential equations,” *Journal of Physics A: Mathematical and Theoretical* **58**, 155304 (2025).

[44] Edward Farhi and Hartmut Neven, “Classification with quantum neural networks on near term processors,” arXiv:1802.06002 (2018).

[45] Adrián Pérez-Salinas, Alba Cervera-Lierta, Elies Gil-Fuster, and José I. Latorre, “Data re-uploading for a universal quantum classifier,” *Quantum* **4**, 226 (2020).

[46] Amira Abbas, Robbie King, Hsin-Yuan Huang, William J. Huggins, Ramis Movassagh, Dar Gilboa, and Jarrod Ryan McClean, “On quantum backpropagation, information reuse, and cheating measurement collapse,” in *Thirty-seventh Conference on Neural Information Processing Systems* (2023).

[47] Iris Cong, Soonwon Choi, and Mikhail D. Lukin, “Quantum convolutional neural networks,” *Nature Physics* **15**, 1273–1278 (2019).

[48] Hsin-Yuan Huang, Richard Kueng, and John Preskill, “Information-Theoretic Bounds on Quantum Advantage in Machine Learning,” *Phys. Rev. Lett.* **126**, 190505 (2021).

[49] Hsin-Yuan Huang, “Learning quantum states from their classical shadows,” *Nature Reviews Physics* **4**, 81–81 (2022).

[50] Shi Jin and Nana Liu, “Analog quantum simulation of parabolic partial differential equations using Jaynes-Cummings-like models,” arXiv preprint arXiv:2407.01913 (2024).

[51] Edward Farhi, Jeffrey Goldstone, and Sam Gutmann, “A Quantum Approximate Optimization Algorithm,” (2014), arXiv.1411.4028; Report no. MIT-CTP/4610.

[52] Abhinav Kandala, Antonio Mezzacapo, Kristan Temme, Maika Takita, Markus Brink, Jerry M. Chow, and Jay M. Gambetta, “Hardware-efficient variational quantum eigensolver for small molecules and quantum magnets,” *Nature* **549**, 242–246 (2017).

Appendix A: Proofs

1. Proof of Lemma 2

Without loss of generality, we can only consider the time-derivative with respect to a particular index m . Given the loss function $\mathcal{L}(\rho(T, \theta))$, the chain rule gives

$$\frac{\partial \mathcal{L}(\rho(T, \theta))}{\partial \theta_m} = \text{tr} \left(\frac{\delta \mathcal{L}(\rho(T, \theta))}{\delta \rho} \sigma_m(T, \theta) \right), \quad (\text{A1})$$

where we define

$$\sigma_m(s, \theta) := \frac{\partial \rho(s, \theta)}{\partial \theta_m}, \quad s \in [0, T]. \quad (\text{A2})$$

To solve for $\sigma_m(T, \theta)$, we write down the dynamics of $\sigma_m(s, \theta)$

$$\begin{aligned} \frac{\partial \sigma_m(s, \theta)}{\partial s} &= \frac{\partial}{\partial \theta_m} \frac{\partial \rho(s, \theta)}{\partial s} = -i \frac{\partial}{\partial \theta_m} [H(s, \theta), \rho(s, \theta)] \\ &= -i[H(s, \theta), \sigma_m(s, \theta)] - i \left[\frac{\partial H(s, \theta)}{\partial \theta_m}, \rho(s, \theta) \right], \quad \sigma_m(0, \theta) = 0, \end{aligned} \quad (\text{A3})$$

where the initial condition $\sigma_m(0, \theta) = 0$ is due to the fact that the initial state ρ_0 is independent of the parameter θ inside Hamiltonians. Note that the homogeneous part of Eq. (A3) has solution $\sigma_m^h(T, \theta) = U_\theta(s, T) \sigma_m^h(s, \theta) U_\theta^\dagger(s, T)$ where $U_\theta(s, T) = \mathcal{T} \exp(-i \int_s^T H(\tau, \theta) d\tau)$. The inhomogeneous part of Eq. (A3) is $-i[\frac{\partial H(s, \theta)}{\partial \theta_m}, \rho(s, \theta)]$, which can be viewed as an additional force term. Either by introducing $U_\theta(s, T)$ as integrating factors or by applying Duhamel’s principle directly, Eq. (A3) can be expressed in the integral

form as follows:

$$\sigma_m(T, \theta) = i \int_0^T U_\theta(s, T) \left[\rho(s, \theta), \frac{\partial H(s, \theta)}{\partial \theta_m} \right] U_\theta^\dagger(s, T) ds. \quad (\text{A4})$$

Inserting Eq. (A4) into Eq. (A1) gives

$$\begin{aligned} \frac{\partial \mathcal{L}(\rho(T, \theta))}{\partial \theta_m} &= i \int_0^T \text{tr} \left(\frac{\delta \mathcal{L}(\rho(T, \theta))}{\delta \rho} U_\theta(s, T) \left[\rho(s, \theta), \frac{\partial H(s, \theta)}{\partial \theta_m} \right] U_\theta^\dagger(s, T) \right) ds \\ &= i \int_0^T \text{tr} \left(U_\theta^\dagger(s, T) \frac{\delta \mathcal{L}(\rho(T, \theta))}{\delta \rho} U_\theta(s, T) \left[\rho(s, \theta), \frac{\partial H(s, \theta)}{\partial \theta_m} \right] \right) ds \\ &= i \int_0^T \text{tr} \left(U_\theta(T, s) \frac{\delta \mathcal{L}(\rho(T, \theta))}{\delta \rho} U_\theta^\dagger(T, s) \left[\rho(s, \theta), \frac{\partial H(s, \theta)}{\partial \theta_m} \right] \right) ds \\ &= i \int_0^T A_T(\theta) \text{tr} \left(a(s, \theta) \left[\rho(s, \theta), \frac{\partial H(s, \theta)}{\partial \theta_m} \right] \right) ds \end{aligned} \quad (\text{A5})$$

where in the last line, we introduce the notation

$$a(s, \theta) := \frac{U_\theta(T, s) \frac{\delta \mathcal{L}(\rho(T, \theta))}{\delta \rho} U_\theta^\dagger(T, s)}{A_T(\theta)}, \quad A_T(\theta) := \text{tr}(\delta \mathcal{L}(\rho(T, \theta)) / \delta \rho).$$

Clearly, the state $a(s, \theta)$ undergoes unitary evolution according to Eq. (24) with a terminal condition, and $\text{tr}(a(s, \theta)) = 1$ is preserved for all $s \in [0, T]$. One can also rewrite

$$\text{tr} \left(a(s, \theta) \left[\rho(s, \theta), \frac{\partial H(s, \theta)}{\partial \theta_m} \right] \right) = \text{tr} \left(\left[\frac{\partial H(s, \theta)}{\partial \theta_m}, a(s, \theta) \right] \rho(s, \theta) \right), \quad (\text{A6})$$

and the results of the lemma follows.

2. Proof of Theorem 3

It is clear that the state

$$\begin{aligned} \eta(s, \theta) &= (|0\rangle\langle 0| \otimes \mathbf{1} \otimes \mathbf{1} + |1\rangle\langle 1| \otimes \mathbf{S}) (|+\rangle\langle +| \otimes a(s, \theta) \otimes \rho(s, \theta)) (|0\rangle\langle 0| \otimes \mathbf{1} \otimes \mathbf{1} + |1\rangle\langle 1| \otimes \mathbf{S}) \\ &= \frac{1}{2} \left(|0\rangle\langle 0| \otimes a(s, \theta) \otimes \rho(s, \theta) + |0\rangle\langle 1| \otimes (a(s, \theta) \otimes \rho(s, \theta)) \mathbf{S} \right. \\ &\quad \left. + |1\rangle\langle 0| \otimes \mathbf{S} (a(s, \theta) \otimes \rho(s, \theta)) + |1\rangle\langle 1| \otimes \rho(s, \theta) \otimes a(s, \theta) \right). \end{aligned}$$

It can be observed that the integrand in Eq. (23) can be written as

$$\begin{aligned} &i A_T(\theta) \text{tr} \left(\left[\frac{\partial H(s, \theta)}{\partial \theta_m}, a(s, \theta) \right] \rho(s, \theta) \right) \\ &= i A_T(\theta) \text{tr} \left(\frac{\partial H(s, \theta)}{\partial \theta_m} a(s, \theta) \rho(s, \theta) - \frac{\partial H(s, \theta)}{\partial \theta_m} \rho(s, \theta) a(s, \theta) \right) \\ &= 2 A_T(\theta) \text{tr} (O_m(s, \theta) \eta(s, \theta)). \end{aligned}$$

To validate the last equality explicitly, let us decompose $\rho(s, \theta) = \sum_k \lambda_k |b_k\rangle\langle b_k|$ and $a(s, \theta) = \sum_k \mu_k |a_k\rangle\langle a_k|$. Then by direct decomposition, one can verify that

$$\begin{aligned} &2 \text{tr} (O_m(s, \theta) \eta(s, \theta)) \\ &= -i \text{tr} \left(\left(\frac{\partial H(s, \theta)}{\partial \theta_m} \otimes \mathbf{1} \right) \mathbf{S} (a(s, \theta) \otimes \rho(s, \theta)) \right) + i \text{tr} \left(\left(\frac{\partial H(s, \theta)}{\partial \theta_m} \otimes \mathbf{1} \right) (a(s, \theta) \otimes \rho(s, \theta)) \mathbf{S} \right) \\ &= -i \sum_{j,k} \mu_j \lambda_k \langle b_k | |a_j\rangle \langle a_j | \frac{\partial H(s, \theta)}{\partial \theta_m} |b_k\rangle + i \sum_{j,k} \mu_j \lambda_k \langle b_k | \frac{\partial H(s, \theta)}{\partial \theta_m} |a_j\rangle \langle a_j | |b_k\rangle \end{aligned}$$

$$\begin{aligned}
&= -i \sum_k \lambda_k \langle b_k | a(s, \theta) \frac{\partial H(s, \theta)}{\partial \theta_m} | b_k \rangle + i \sum_k \langle b_k | \frac{\partial H(s, \theta)}{\partial \theta_m} a(s, \theta) | b_k \rangle \\
&= -i \text{tr} \left(\frac{\partial H(s, \theta)}{\partial \theta_m} \rho(s, \theta) a(s, \theta) \right) + i \text{tr} \left(\frac{\partial H(s, \theta)}{\partial \theta_m} a(s, \theta) \rho(s, \theta) \right).
\end{aligned}$$

Thus the proof is complete.

3. Proof of Theorem 5

The eigenstates $\{|s\rangle\}_{s \in \mathbb{R}}$ form an orthonormal basis with $\int |s\rangle \langle s| ds = \mathbf{1}_s$ and the position operator $\hat{s} := \int s |s\rangle \langle s| ds$. Recall from Eq. (27) that

$$\hat{\eta}(\theta) = \int g(s) |s\rangle \langle s| \otimes \eta(s, \theta) ds, \quad \int g(s) ds = 1,$$

By confining to time-independent Hamiltonians, the operator (from Theorem 3) $O_m(s, \theta) \rightarrow O_m(\theta)$ is independent of s . Then one easily observes that

$$\text{tr}((\mathbf{1}_s \otimes O_m(\theta)) \hat{\eta}(\theta)) = \int g(s) \text{tr}(O_m(\theta) \eta(s, \theta)) ds$$

When $g(s) = g_{top}(s)$, then clearly $\int g(s) \text{tr}(O_m(\theta) \eta(s, \theta)) ds = \frac{1}{T} \int_0^T \text{tr}(O_m(\theta) \eta(s, \theta)) ds$.

Proof for the error bounds of imperfect $g(s)$:

Since the quantum $\int g_{top}(s) |s\rangle \langle s| ds$ cannot be exactly prepared (if we keep s continuous) due to discontinuity at $s = 0$ and $s = T$, we instead approximate it using a quemode $\int g(s) |s\rangle \langle s| ds$. By Eq. (29) and the triangle inequality,

$$\begin{aligned}
&\left| \frac{1}{2TA_T(\theta)} \frac{\partial \mathcal{L}_\theta}{\partial \theta_m} - \text{tr}(\mathbf{1}_s \otimes O_m(\theta) \hat{\eta}(\theta)) \right| \\
&\stackrel{(29)}{=} \left| \text{tr} \left(\mathbf{1}_s \otimes O_m(\theta) \int (g_{top}(s) - g(s)) |s\rangle \langle s| \otimes \eta(s, \theta) ds \right) \right| \\
&= \left| \int (g_{top}(s) - g(s)) d\text{str}(O_m(\theta) \eta(s, \theta)) \right| \\
&\leq \int |g_{top}(s) - g(s)| |\text{tr}(O_m(\theta) \eta(s, \theta))| ds.
\end{aligned}$$

Since $\eta(s, \theta)$ is a density matrix which is positive semi-definite and $\text{tr}(\eta(s, \theta)) = 1$, one has

$$|\text{tr}(O_m(\theta) \eta(s, \theta))| \leq \|O_m(\theta)\|_\infty,$$

where $\|O_m(\theta)\|_\infty$ is the operator norm of $O_m(\theta)$, or equivalently, the largest eigenvalue of $|O_m(\theta)|$. Therefore,

$$\begin{aligned}
&\left| \frac{1}{2TA_T(\theta)} \frac{\partial \mathcal{L}_\theta}{\partial \theta_m} - \text{tr}(\mathbf{1}_s \otimes O_m(\theta) \hat{\eta}(\theta)) \right| \\
&\leq \|O_m(\theta)\|_\infty \int |g_{top}(s) - g(s)| ds \\
&= \|O_m(\theta)\|_\infty \|g_{top} - g\|_{\text{TV}}.
\end{aligned}$$

Proof for the realization for time-independent case:

$$\hat{\eta}(\theta) \stackrel{(27)}{=} \int g(s) |s\rangle \langle s| \otimes \eta(s, \theta) ds$$

$$\begin{aligned}
&= \int g(s)|s\rangle\langle s| \otimes \mathcal{V}_\theta(s)\eta(0, \theta)\mathcal{V}_\theta(s)^\dagger ds \\
&\stackrel{(26)}{=} \int g(s)|s\rangle\langle s| \otimes \mathcal{C}_{\text{swap}}(\mathbf{1} \otimes e^{iH(\theta)(T-s)} \otimes e^{-iH(\theta)s})\eta(0, \theta)(\mathbf{1} \otimes e^{-iH(\theta)(T-s)} \otimes e^{iH(\theta)s})\mathcal{C}_{\text{swap}} ds \\
&= (\mathbf{1}_s \otimes \mathcal{C}_{\text{swap}})W\left(\int g(s)|s\rangle\langle s| \otimes \eta(0, \theta)ds\right)W^\dagger(\mathbf{1}_s \otimes \mathcal{C}_{\text{swap}}),
\end{aligned}$$

where the unitary gate W acting on the s -mode, auxillary qubit \mathcal{H}_{aux} , the adjoint mode \mathcal{H}_{adj} and the original mode \mathcal{H} , consists of the application of two unitary gates sequentially

$$W = (\mathbf{1}_{\mathcal{H}_{\text{aux}}} \otimes e^{-iH(\theta) \otimes \hat{s}} \otimes \mathbf{1}_{\mathcal{H}_{\text{adj}}})(\mathbf{1}_{\mathcal{H}_{\text{aux}}} \otimes e^{iH(\theta) \otimes (T\mathbf{1}_s - \hat{s})} \otimes \mathbf{1}_{\mathcal{H}}).$$

Appendix B: Complexity scaling of quantum measurements for Section IV D

Let us denote the time-discretised expression in Eq. (33) as

$$\mathcal{I}_m := \sum_{j=1}^{N_t} \sum_{k=1}^K \Delta s \frac{\partial f_k(s_j, \theta)}{\partial \theta_m} \text{tr}(\sigma_Y \otimes H_k \otimes \mathbf{1} \eta(s_j, \theta)).$$

For simplicity, we shall simply choose the midpoint rule with $\Delta s = \frac{T}{N_t}$. Suppose we use L samples to estimate the quantum observable $\text{tr}(\sigma_Y \otimes H_k \otimes \mathbf{1} \eta(s_j, \theta))$ for each k and j , and let its quantum measurement outcome be $X_{k,j}$, which are independent random variables. Let

$$\mathcal{X}_m := \sum_{j=1}^{N_t} \sum_{k=1}^K \Delta s \frac{\partial f_k(s_j, \theta)}{\partial \theta_m} X_{k,j},$$

which is an unbiased estimator of \mathcal{I}_m .

We make the following assumptions, which are not very restrictive:

Assumption 7. *Without loss of generality, we assume that each term H_k has operator norm $\|H_k\|_\infty = 1$. Suppose that for each $s \in [0, T]$ and index $1 \leq k \leq K$, $1 \leq m \leq M$, we have uniform bounds for the following:*

$$|f_k(s, \theta)|, \left|\frac{\partial f_k(s, \theta)}{\partial s}\right|, \left|\frac{\partial f_k(s, \theta)}{\partial \theta_m}\right|, \left|\frac{\partial^2 f_k(s, \theta)}{\partial \theta_m \partial s}\right|, \left|\frac{\partial^3 f_k(s, \theta)}{\partial \theta_m \partial s^2}\right| \leq \alpha.$$

We will need the following lemma about the moment generating function for quantum measurements:

Lemma 8. *Under Assumption 7, we fix each k and j , then for each $X \equiv X_{k,j}$, its moment generating function is bounded by*

$$\mathbb{E}(e^{\lambda(X - \mathbb{E}(X))}) \leq e^{\frac{\lambda^2}{2L^2}}, \quad \forall \lambda \in \mathbb{R}.$$

Proof. Suppose Y_1, Y_2, \dots, Y_L are i.i.d. random samples for X , then due to the given assumptions, we know that $Y_i \in [-1, 1]$. The estimator $X = \frac{1}{L} \sum_{i=1}^L Y_i$ is the average. By independence of Y_i , we have

$$\mathbb{E}(e^{\lambda(X - \mathbb{E}(X))}) = \prod_{i=1}^L \mathbb{E}(e^{\frac{\lambda}{L}(Y_i - \mathbb{E}(Y_i))}) \leq \prod_{i=1}^L e^{\frac{\lambda^2}{2L^2}} = e^{\frac{\lambda^2}{2L}},$$

where we used Hoeffding's lemma to obtain the above inequality. \square

Lemma 9. *Under Assumption 7, for each fixed m ,*

$$\mathbb{E}\left[e^{\lambda \left|\sum_{j=1}^{N_t} \sum_{k=1}^K \Delta s \frac{\partial f_k(s_j, \theta)}{\partial \theta_m} (X_{k,j} - \mathbb{E}(X_{k,j}))\right|}\right] \leq 2 \exp\left(\frac{\lambda^2 T^2 \alpha^2 K}{2N_t L}\right).$$

Proof. This conclusion can be obtained by the last lemma:

$$\begin{aligned}
& \mathbb{E} \left[e^{\lambda \left| \sum_{j=1}^{N_t} \sum_{k=1}^K \Delta s \frac{\partial f_k(s_j, \theta)}{\partial \theta_m} (X_{k,j} - \mathbb{E}(X_{k,j})) \right|} \right] \\
& \leq \mathbb{E} \left[e^{\lambda \sum_{j=1}^{N_t} \sum_{k=1}^K \Delta s \frac{\partial f_k(s_j, \theta)}{\partial \theta_m} (X_{k,j} - \mathbb{E}(X_{k,j}))} \right] + \mathbb{E} \left[e^{-\lambda \sum_{j=1}^{N_t} \sum_{k=1}^K \Delta s \frac{\partial f_k(s_j, \theta)}{\partial \theta_m} (X_{k,j} - \mathbb{E}(X_{k,j}))} \right] \\
& \leq \prod_{j=1}^{N_t} \prod_{k=1}^K e^{\lambda \Delta s \frac{\partial f_k(s_j, \theta)}{\partial \theta_m} (X_{k,j} - \mathbb{E}(X_{k,j}))} + \prod_{j=1}^{N_t} \prod_{k=1}^K e^{-\lambda \Delta s \frac{\partial f_k(s_j, \theta)}{\partial \theta_m} (X_{k,j} - \mathbb{E}(X_{k,j}))} \\
& \leq 2 \prod_{j=1}^{N_t} \prod_{k=1}^K \exp \left(\frac{(\lambda \Delta s \frac{\partial f_k(s_j, \theta)}{\partial \theta_m})^2}{2L} \right) \leq 2 \prod_{j=1}^{N_t} \prod_{k=1}^K \exp \left(\frac{(\lambda \Delta s \alpha)^2}{2L} \right) = 2 \exp \left(\frac{\lambda^2 T^2 \alpha^2 K}{2N_t L} \right).
\end{aligned}$$

□

Then we have the following conclusion:

Proposition 10. *Under Assumption 7,*

(i) *Suppose that we choose midpoint scheme with uniform grid points for Eq. (33). We only need to choose*

$$N_t \geq \mathcal{O}(T^{3/2} K^{3/2} \delta^{-1/2}),$$

then one could ensure that $\left| \frac{1}{2A_T(\theta)} \frac{\partial \mathcal{L}_\theta}{\partial \theta_m} - \mathcal{I}_m \right| \leq \delta/2$ for any $1 \leq m \leq M$.

(ii) *To ensure that*

$$\mathbb{P} \left(\max \left| \mathcal{X}_m - \frac{1}{2A_T(\theta)} \frac{\partial \mathcal{L}_\theta}{\partial \theta_m} \right| \geq \delta \right) \leq \varepsilon, \quad 1 \leq m \leq M$$

it is sufficient to choose the total number of quantum measurements as

$$\max \left\{ \mathcal{O}(T^2 K^2 \delta^{-2} \log(\frac{M}{\varepsilon})), \mathcal{O}(T^{3/2} K^{5/2} \delta^{-1/2}) \right\}.$$

Proof. Proof of part (i):

$$\frac{1}{2A_T(\theta)} \frac{\partial \mathcal{L}_\theta}{\partial \theta_m} = \int_0^T \text{tr}(O_m(s, \theta) \eta(s, \theta)) ds = \sum_{k=1}^K \int_0^T \frac{\partial f_k(s, \theta)}{\partial \theta_m} \text{tr}(\sigma_Y \otimes H_k \otimes \mathbf{1} \eta(s, \theta)) ds.$$

To ensure that the error from time-discretization is bounded by $\delta/2$, it is sufficient to ensure that the midpoint scheme for each term k has error

$$\left| \int_0^T \frac{\partial f_k(s, \theta)}{\partial \theta_m} \text{tr}(\sigma_Y \otimes H_k \otimes \mathbf{1} \eta(s, \theta)) ds - \sum_{j=1}^{N_t} \Delta s \frac{\partial f_k(s_j, \theta)}{\partial \theta_m} \text{tr}(\sigma_Y \otimes H_k \otimes \mathbf{1} \eta(s_j, \theta)) \right| \leq \frac{\delta}{2K}.$$

We can directly verify that for $h(s, \theta) = \frac{\partial f_k(s, \theta)}{\partial \theta_m} \text{tr}(\sigma_Y \otimes H_k \otimes \mathbf{1} \eta(s, \theta))$, its second-order derivative with respect to time is bounded by

$$\begin{aligned}
\left| \frac{\partial^2 h(s, \theta)}{\partial s^2} \right| & \leq \left| \frac{\partial^3 f_k(s, \theta)}{\partial \theta_m \partial s^2} \text{tr}(\sigma_Y \otimes H_k \otimes \mathbf{1} \eta(s, \theta)) \right| \\
& + 2 \left| \frac{\partial^2 f_k(s, \theta)}{\partial \theta_m \partial s} \text{tr}(\sigma_Y \otimes H_k \otimes \mathbf{1} \partial_s \eta(s, \theta)) \right| \\
& + \left| \frac{\partial f_k(s, \theta)}{\partial \theta_m} \text{tr}(\sigma_Y \otimes H_k \otimes \mathbf{1} \partial_s^2 \eta(s, \theta)) \right| \\
& \leq \alpha + 2\alpha |\text{tr}(\sigma_Y \otimes H_k \otimes \mathbf{1} \partial_s \eta(s, \theta))| + \alpha |\text{tr}(\sigma_Y \otimes H_k \otimes \mathbf{1} \partial_s^2 \eta(s, \theta))|
\end{aligned}$$

$$\begin{aligned} &\leq \alpha + 2\alpha(2\alpha K) + \alpha(2\alpha K + 4\alpha^2 K^2) \\ &\leq \alpha(1 + 3\alpha K)^2. \end{aligned}$$

Therefore, it is easy to show that for the midpoint scheme with step size Δs , the time-discretization error is bounded by

$$\frac{1}{24} \Delta s^2 T \alpha (1 + 3\alpha K)^2,$$

which is required to be smaller than $\frac{\delta}{2K}$. Then it is easy to show that

$$N_t \geq \sqrt{\frac{T^3 \alpha (1 + 3\alpha K)^2 K}{12\delta}} = \mathcal{O}(T^{3/2} K^{3/2} \delta^{-1/2}).$$

Proof of part (ii): We assume that the conclusion in part (i) holds as a starting point. By triangle inequality, we obtain

$$\begin{aligned} &\mathbb{P}\left(\max_{m=1}^M \left| \mathcal{X}_m - \frac{1}{2A_T(\theta)} \frac{\partial \mathcal{L}_\theta}{\partial \theta_m} \right| \geq \delta\right) \\ &\leq \mathbb{P}\left(\max_{m=1}^M |\mathcal{X}_m - \mathcal{I}_m| \geq \delta/2\right) \\ &\leq \sum_{m=1}^M \mathbb{P}\left(|\mathcal{X}_m - \mathcal{I}_m| \geq \delta/2\right) \\ &= \sum_{m=1}^M \mathbb{P}\left(\left| \sum_{j=1}^{N_t} \sum_{k=1}^K \Delta s \frac{\partial f_k(s_j, \theta)}{\partial \theta_m} (X_{k,j} - \mathbb{E}(X_{k,j})) \right| \geq \delta/2\right) \\ &\leq \sum_{m=1}^M e^{-\lambda \delta/2} \mathbb{E}\left[e^{\lambda \left| \sum_{j=1}^{N_t} \sum_{k=1}^K \Delta s \frac{\partial f_k(s_j, \theta)}{\partial \theta_m} (X_{k,j} - \mathbb{E}(X_{k,j})) \right|}\right] \quad (\text{Markov inequality for any } \lambda > 0) \\ &\leq 2M e^{-\lambda \delta/2} \exp\left(\frac{\lambda^2 T^2 \alpha^2 K}{2N_t L}\right). \end{aligned}$$

By optimizing the upper bound over all λ , we have

$$\mathbb{P}\left(\max_{m=1}^M \left| \mathcal{X}_m - \frac{1}{2A_T(\theta)} \frac{\partial \mathcal{L}_\theta}{\partial \theta_m} \right| \geq \delta\right) = 2M \exp\left(-\frac{\delta^2}{16A}\right), \quad A = \frac{T^2 \alpha^2 K}{2N_t L}.$$

Since we want the probability to be less than ε , we require

$$N_t L K \geq 8T^2 \alpha^2 K^2 \delta^{-2} \log\left(\frac{2M}{\varepsilon}\right) = \mathcal{O}(T^2 K^2 \delta^{-2} \log\left(\frac{M}{\varepsilon}\right)),$$

where $N_t L K$ is the number of measurements required to estimate $\partial \mathcal{L}_\theta / \partial \theta_m$. L is the number of copies of the state required to compute the expectation value of $X_{k,j}$, for each (k, j) pair, so that the gradient of the loss function can be estimated to high precision with high probability, and there are $N_t K$ such pairs.

By part (i), we require $L \geq 1$, so that

$$N_t L K \geq \mathcal{O}(T^{3/2} K^{5/2} \delta^{-1/2}).$$

By combining the above results, we obtain

$$\max \left\{ \mathcal{O}(T^2 K^2 \delta^{-2} \log\left(\frac{M}{\varepsilon}\right)), \mathcal{O}(T^{3/2} K^{5/2} \delta^{-1/2}) \right\}.$$

□

Appendix C: Supplemental details for Section V

1. Hamiltonians used in numerical experiments

Hamiltonian of H_2 molecule:

During numerical experiments, we use the following Hamiltonian representation for hydrogen molecule from [52]:

$$H_{\text{hydro}} = 0.397936 \sigma_Z^{(1)} + 0.397936 \sigma_Z^{(2)} + 0.011280 \sigma_Z^{(1)} \otimes \sigma_Z^{(2)} + 0.180931 \sigma_X^{(1)} \otimes \sigma_X^{(2)}. \quad (\text{C1})$$

The Hamiltonian has been mapped into the representation of two qubits.

Quantum Ising chain:

We consider the Hamiltonian learning problem from [24]. The parameterised Hamiltonian is chosen as 1D Ising chain with L sites herein:

$$H = \sum_{i=1}^{L-1} x_i \sigma_Z^{(i)} \otimes \sigma_Z^{(i+1)}. \quad (\text{C2})$$

The parameters x_i are randomly initiated from $[-0.5, -0.08] \cup [0.08, 0.5]$ similarly to [24]. The initial state is chosen as $|+\rangle^{\otimes L}$ followed by possible random rotation (see Table II).

Time-dependent quantum Ising chain:

We also consider the time-dependent case:

$$H = \sum_{i=1}^{L-1} x_i \sigma_Z^{(i)} \otimes \sigma_Z^{(i+1)} + f(t) \sum_{i=1}^L \sigma_X^{(i)}, \quad (\text{C3})$$

where $f(t) = \sin(\pi t)$ for experiments in Section V. For ansatz, we consider the same structure as the above, and train the model to learn x_i and $f(t)$. For the function $f(t)$, we use a two-layer network with sin function as the activation function, namely, $f(t) \approx f_\theta(t) = \sum_{k=1}^m w_k^{(2)} \sin(w_k^{(1)} t + b_k) + b$ where the parameter θ is simply the collection $\{w_k^{(2)}\}_{k=1}^m$, $\{w_k^{(1)}\}_{k=1}^m$, $\{b_k\}_{k=1}^m$, and b . For the above experiments, we simply pick $m = 2$ for simplicity.

2. Decomposition of Pauli matrices in adjoint states

It is easy to validate the following decompositions:

$$\begin{aligned} \sigma_Z &= |0\rangle\langle 0| - |1\rangle\langle 1| \\ \sigma_X &= |+\rangle\langle +| - |-\rangle\langle -|, \quad |\pm\rangle = \frac{1}{\sqrt{2}}(|0\rangle \pm |1\rangle) \\ \sigma_Y &= |\psi_1\rangle\langle\psi_1| - |\psi_2\rangle\langle\psi_2|, \quad \psi_1 = \frac{1}{\sqrt{2}}(|1\rangle - i|0\rangle), \quad \psi_2 = \frac{1}{\sqrt{2}}(|1\rangle + i|0\rangle). \end{aligned}$$

All these pure states are easy to prepare. For two-body Pauli matrice $\sigma_X \otimes \sigma_Y$ as an example, one can decompose it into the summation of 4 terms:

$$\begin{aligned} \sigma_X \otimes \sigma_Y &= (|+\rangle\langle +| \otimes |\psi_1\rangle\langle\psi_1|) - (|+\rangle\langle +| \otimes |\psi_2\rangle\langle\psi_2|) \\ &\quad - (|-\rangle\langle -| \otimes |\psi_1\rangle\langle\psi_1|) + (|-\rangle\langle -| \otimes |\psi_2\rangle\langle\psi_2|). \end{aligned}$$

Therefore, one can run the optimisation algorithm for the Hamiltonian learning using loss function in Eq. (10), for all observables constructed via the tensor product of local Pauli matrices.

3. Details of training

Optimisation - The training hyper-parameters are summarized in the following Table II. For the toy model of learning unknown state, we simply use the stochastic gradient descent method; for other problems, we use the Adam method for the parameter update (together with batch samples). For the integral in Eq. (25), we always discretise it using the Trapezoidal rule; for the mixed state simulation, we use the first-order Trotter splitting to simulate $U_\theta(s, t)$ in Eq. (26) for any initial and terminal time s, t . For the mixed state simulation for the loss function in Eq. (10), the choice of observables as well as whether to randomize the observables play a non-trivial role in the efficiency and training accuracy, which is also a challenging topic in quantum state tomography. A more comprehensive study on the optimal way to choose the classical training procedure will be interesting for future endeavors.

Test error - In the above experiments in Section V, we always report 1 – Fidelity which is defined as follows:

$$1 - \frac{1}{M_s} \sum_{i=1}^{M_s} |\langle \phi_i | U_\theta^\dagger(0, T_i) U(0, T_i) | \phi_i \rangle|^2 \quad (\text{C4})$$

where T_i are possibly randomly generated (see Table II), the initial state $\rho_i = |\phi_i\rangle\langle\phi_i|$ are generated randomly by applying

$$|\phi_i\rangle = \text{RZ}(\alpha) \text{RY}(\beta) \text{RX}(\gamma) |+\rangle, \quad \alpha, \beta, \gamma \sim \text{Uniform}(0, 4\pi).$$

The unitary $U(0, T)$ is the exact unitary evolution of the black-box Hamiltonian from time zero to T and $U_\theta(0, T)$ is the unitary for parameterised Hamiltonian. In all experiments, we choose $M_s = 50$. All gates and observables are implemented in the syntax of PennyLane.

TABLE II: Below are key hyper-parameters for the training.

Loss function	lr	initialization ρ_i	T_i	batch size of (ρ_i, T_i)	Figure
Eq. (8)	10^{-2}	$ 0\rangle$	1	n/a	Fig. 2
Eq. (9) for Hydrogen	10^{-2}	$ +\rangle^{\otimes n}$	Uniform(1, 2)	1	Fig. 3
Eq. (9) for Ising	10^{-2}	$ +\rangle^{\otimes n}$	Uniform(1, 2)	1	Fig. 3
Eq. (9) for time-dependent Ising	2×10^{-2}	$ +\rangle^{\otimes n}$ with random rotation	Uniform(1, 2)	10	Fig. 4
Eq. (10) for Hydrogen	8×10^{-3}	$ +\rangle^{\otimes n}$ with random rotation	Uniform(1, 2)	1	Fig. 5a
Eq. (10) for Ising	8×10^{-3}	$ +\rangle^{\otimes n}$ with random rotation	Uniform(1, 2)	1	Fig. 5a
Eq. (10) for time-dependent Ising	2×10^{-2}	$ +\rangle^{\otimes n}$ with random rotation	Uniform(1, 2)	10	Fig. 5b